A FEASIBILITY STUDY OF TWO ALTERNATE PROTON RADIATION COMPENSATOR DESIGNS FOR USE IN PROTON RADIATION THERAPY

By

Johnathan Tyler Bennett

A Thesis
Submitted to the
Faculty of the Graduate School
of
Western Carolina University
in Partial Fulfillment of the
Requirements for the degree
of
Master of Science in Technology.

Committee:

_____ Director

_____

_____

_____ Dean of the Graduate School

Date: _____

Summer 2010
Western Carolina University
Cullowhee, North Carolina

A FEASIBILITY STUDY OF TWO ALTERNATE PROTON RADIATION COMPENSATOR DESIGNS FOR USE IN PROTON RADIATION THERAPY

A thesis presented to the faculty of the Graduate School of Western Carolina University in partial fulfillment of the requirements for the degree of Master of Science in Technology.

By

Johnathan Tyler Bennett

Director:

Dr. Chip Ferguson

Committee Members:

Dr. Phillip Sanger

Dr. Wes Stone

June 2010

Acknowledgements

I would like to thank my committee, Dr. Ferguson, Dr. Sanger, and Dr. Stone for their insight and encouragement during this research. Richard Helmig and his associates in the Shands Radiation Oncology Department at the University of Florida for being extremely helpful and permitting the use of their radiation facilities. And a whole-hearted thanks to my fellow graduate students for their assistance and positive reinforcement during my extensive research.

TABLE OF CONTENTS

LIST OF FIGURES

ABSTRACT

The purpose of the current thesis was to conduct a feasibility study of alternate methods for creating proton range compensators. Currently, proton range compensators are made of solid materials, but an interest in creating a proton range compensator using fluid has arose in respect to a need for cost and time efficiency. The current process of making proton compensators is costly and time consuming. A fluid-based design is expected to allow doctors to quickly "dial up" a dose within a matter of minutes. The current study included the fabrication, and testing, of a fluid-based range compensator. The fluid-based design consisted of a block of acrylic with an array of holes. Each of the holes was plugged with an acrylic plunger. The plungers were depressed to a desired depth to achieve a specific dosimetric value. The testing sequence used in the current study included multiple compensator configurations that were used to compare the fluid-based design to the conventional solid design. Photon radiation was passed through each compensator and each compensator's exposure image was compared. The results of the statistical analysis showed no significant similarities between the conventional compensator design and the fluid-based compensator design. Reflection of the current study discusses the potential for the fluid-based design to be used as an alternative method to achieve proton range compensation rather than a replacement for the conventional solid design.

CHAPTER 1: STATEMENT OF THE PROBLEM

1.1 Objective

The objective of the current thesis research effort was to determine the feasibility of using an adjustable water-filled proton radiation compensator design in place of conventional designs that are currently implemented in the field of proton radiation therapy.

1.2 Purpose

The purpose of the current thesis was to conduct a feasibility study of alternate methods for creating proton compensators. Currently, proton range compensators are made of solid materials, but an interest in creating a proton range compensator using fluid has arose in respect to a need for cost and time efficiency. Proton radiation therapy in the treatment of cancer is becoming more popular as patients become aware of the superiority of proton radiation treatment over traditional radiation therapy. In 2006, a proton radiation center in Florida recorded that eighty percent of their patients were self-referred after comparing the benefits of proton radiation therapy to those of conventional radiation therapy (Freeman, 2007). An increase in demand for proton radiation therapy has resulted in a drive for new technologies that allow for more patients to be treated; and at a more economical price. Ion Beam Applications (IBA), the world-leader in the sales of proton radiation equipment (holding sixty percent of global sales in 2007), has invested millions of dollars to increase their employee base in preparation for an extensive expansion in production (Freeman, 2007). During an interview with IBA's founder and chief research officer Yves Jongen, Medical Physics Web's editor Tami Freeman noted that Jongen reported the presence of twenty-two proton therapy centers

worldwide that treat a patient capacity of approximately fifty-thousand patients annually. Freeman continued to note Jongen as he told her that between the years of 1994 and 2005 fourteen industrial contracts were signed pertaining to the development of proton therapy centers. In 2006 four additional proton facility contracts were signed. IBA anticipates the climbing demand to increase to the point that proton therapy makes a transition from a marginal technology to the mainstream method for radiation treatment (Freeman, 2007). With high expectations to redefine the standard for radiation therapy, proton radiation is expected to become readily available at more treatment centers to satisfy demand.

While collaborating with the University of Florida and Shand's Cancer Center, a team of Western Carolina University's (WCU) engineering personnel discussed an interest in designing a proton compensator that can be quickly adjusted to meet the needs of various patients' prescribed radiation treatments. While visiting the proton facilities in Jacksonville, Florida, WCU's engineers noted the current method for creating proton compensators consisted of machining blocks of Lucite to meet pre-determined geometry specified by a radiation physicist. The current method for creating proton compensators takes a minimum of 35-75 minutes for smaller compensators. Larger compensators sometimes take up to several hours to fabricate. Richard Helmig, a reputed medical tooling designer and fabricator working in conjunction with the University of Florida, explained that proton radiation experts agree that a more timely method for creating proton compensators would be highly valued in the field (R. Helmig, personal communication, April, 2009). In respect to the need for a more cost and time-effective compensator, speculation of using a fluid-based compensator to replace the conventional

proton compensator has developed. The current thesis conducted an experiment to determine how well a fluid-based proton compensator can be manufactured and perform in comparison with the conventional proton compensator.

1.3 Background

Proton therapy attracts patients who seek the technology's ability to treat malignant structures that are essentially untreatable by conventional radiation therapy (Chui, 2008). Some areas within the human body, such as the brain or eye, can only tolerate low levels of radiation passing through the healthy tissue. Chui explains that proton radiation can be controlled in such a way that only the targeted area is affected; and the healthy tissue only receives insignificant amounts of radiation, if any. In addition to malignant conditions, conventional proton therapy is used to treat benign conditions by serving as a preventative, or therapeutic, measure for a patient. The use of proton therapy is better than conventional radiation therapy because proton therapy can be used to treat a targeted area without harming the good tissues surrounding the target (The National Association for Proton Therapy, 2009). Proton therapy functions similar to a depth-charge; in that the radiation from the proton can be manipulated to enter a patient's body and reach a certain depth (at the targeted area) prior to emitting an aggressive dose of radiation. According to The Association for Proton Therapy, the depth at which a charged particle, such as a proton, emits the intended dose of energy depends on the speed at which particle is traveling. Charged particles that pass through a body lose speed at specific rates depending on the densities of the tissues (bones, organs, and other tissues) that the particles pass through. The slowing effect is the result of atomic interactions between the particles and the medium that the particles are passing through.

As a particle slows down, the amount of exposure time is increased to allow for a maximum dose deposition (Jäkel, 2009). Jäkel argued that the intended goal behind particle radiation therapy is to manipulate the particles to slow at a rate that allows the maximum dose deposition to be deposited in the target area. The "depth" of emission is calculated using dosimetry. Dosimetry implements the use of three-dimensional (3D) scanning via magnetic resonance imaging (MRI) and computed axial tomography (CAT) scans (University of Florida, Proton Therapy Institute, 2006). MRIs and CAT scans allow doctors to see tumors in 3D. The use of 3D images is currently being used to focus the radiation onto the target area (the tumor) in order to minimize damage to healthy body tissues that surround the target area (Chui, 2008). A visual comparison of the dose delivery between proton radiation and conventional x-ray radiation is shown in *Figure 1.1*. Proton therapy requires each patient to have a unique radiation compensator designed for the shape and location of his/her specific tumor. A compensator acts like a depth-controller for the radiation. Radiation is fired through the compensator in order to deliver a certain amount of energy to the proper area within a patient's body. The range compensator is built dosimetrically in conjunction with the shape, and depth, of the tumor (C. Liu, PH.D., personal communication, April, 2009).

The advantage of proton radiation therapy over conventional x-ray radiation is additionally shown in *Figure 1.1*. The upper line represents the dose-delivery using x-ray radiation. The lower line represents particle radiation (proton radiation is a type of particle radiation). The shaded rectangular area represents a tumor in a body. The tumor is at a particular depth within the body, and requires a certain amount of radiation to reach that particular depth. X-ray radiation has a much larger effect on healthy cells

where proton radiation has a minute effect on healthy cells (Advanced Cancer Therapy Foundation, 2006).

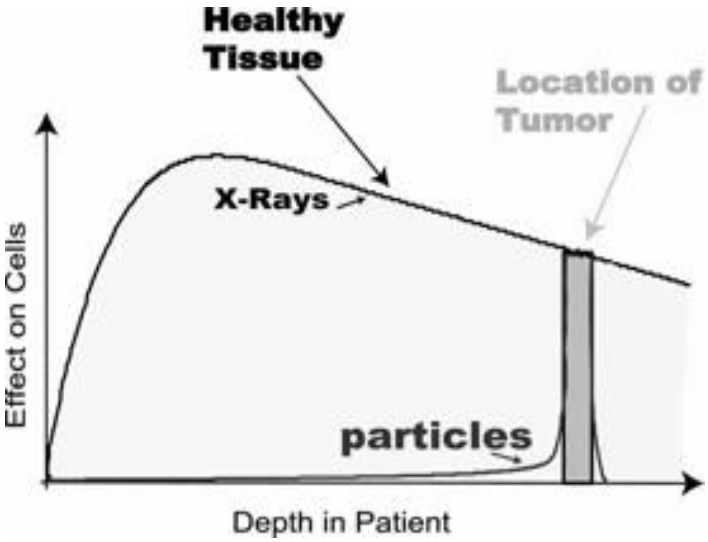

Figure 1.1: The advantage of proton therapy's targeting ability. Online, Advanced Cancter Therapy Foundation, Oct. 2009 <http://www.advanced-cancer-therapy.org/science_radio.html>

The current procedure for creating a custom radiation compensator at the University of Florida Proton Therapy Institute requires doctors to outsource to a machine shop. The process of making proton compensators is costly and time consuming (C. Liu, Ph.D., personal communication, April, 2009). In situations where a tumor is extremely progressive, a doctor may have problems with the time necessary for a compensator to be fabricated. Richard Helmig, a medical tooling expert at the University of Florida, explained that proton therapy facilities have the capability to make a portion of their prescribed compensators in-house, but a large percentage of compensators are outsourced. The smaller compensators, such as those used for prostate cancer patients,

can typically be fabricated in 35-75 minutes (R. Helmig, personal communication, May, 2009). But when outsourced, compensators may take up to several days to be fabricated and delivered. In some cases, a patient may undergo a 3D scan in preparation for radiotherapy only to be disappointed to learn the tumor has progressed into a different shape before the compensator could be fabricated for treatment. A fluid-based design is expected to allow doctors to quickly "dial up" a dose within a matter of minutes. Though the fluid-based design concept seems feasible, no physical groundwork has currently been documented that indicates a fluid-based proton compensator is feasible (R. Helmig, personal communication, April, 2009). The fluid based concept needs to be proved effective in real-world tests to validate theoretical speculation.

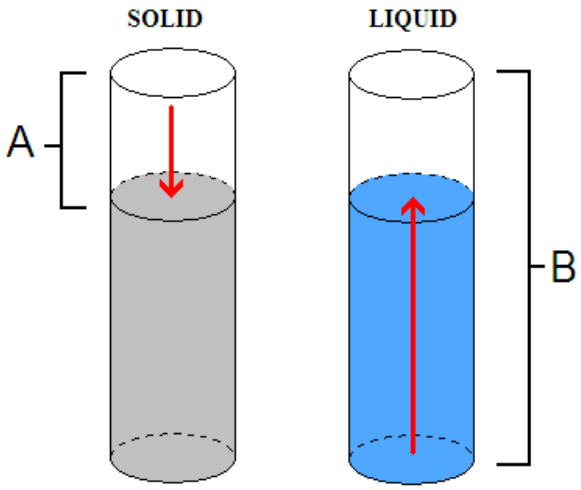

Figure 1.2: Solid design versus liquid design

Figure 1.2, section A, depicts the current technology used to produce a patient-specific proton range compensator. The current method consists of materials being milled down to specific depths to meet the needs of each unique patient. The material

that is machined away is discarded as waste material; as well as the final product after it is used for patient treatment.

Figure 1.2, section B, depicts the proposed fluid-based design for a proton range compensator. A fluid-based compensator would call for an empty chamber to be filled to a specified height to meet the needs of each unique patient. No material is wasted during the filling process; and the process could be performed quicker than the conventional machining method.

1.4 Definitions of Key Terms

Acrylic – a glass-like thermo-polymer favored by radiation experts due to water-like tendencies when exposed to radiation.

Benign – descriptive of an non-normal cell structure that has no threat on a person's health condition.

Bragg peak – the distinct increase in energy that is released from a proton particle as the proton slows and stops at the end of a projected path.

Carbon ion therapy – a type of heavy ion therapy that implements the use of particles from carbon atoms.

CNC – computerized numerical control; a code-based language that is used to control machinery such as mills and lathes.

Dosimetry – refers to the measurement and calculation of a dose of radiation.

External beam radiotherapy – a non-invasive therapy that consists of emitting radiation energy from a source outside of a body with the goal of killing unwanted cell structures.

Heavy ion therapy – similar to proton therapy, heavy ion therapy uses atomic particles that are heavier than protons to combat unwanted cell structures.

Hot Spots – a reference to the areas, on the radiation exposure images, that are found to have an increased amount of radiation than the surrounding area while existing on a uniform specimen thickness.

Internal radiotherapy – an invasive form of radiotherapy that involves emitting radiation from a device inside of a patient.

Irradiate – to expose to radiation.

Lucite® – DuPont™'s trade-name for acrylic.

Malignant – descriptive of a non-normal cell structure that is dangerous to a person's health, and is often progressive in growth.

Milling machine – a piece of equipment used to shape a piece of medium into a desired shape.

OEM – meaning "original equipment manufacturer;" refers to a product that is bought and not made custom.

Particle beam therapy – a form of radiation therapy that consists of generating and controlling atomic particles in such a way as to combat unwanted cell structures.

Proton therapy – a treatment option for various cancerous conditions that implements the use of accelerated proton particles to target any unwanted cell structures.

Protons – positive-charged atomic particles that are used in proton therapy to kill cancerous cells.

Specimen – a reference to an individual compensator. For example, "specimen 1" can be used interchangeably as "compensator 1."

1.5 Limitations & Delimitations of the Study

The current feasibility study was limited to the following criterion:

- Mechanical Design – The feasibility of implementing a fluid-based design through the use chambers, or columns, of water with a circular cross section was considered for the current study. Tolerances of mechanical parts used in the current study are limited to current ability and precision of OEM parts purchased and to the precision capabilities of the machines, and the associated operators, at Western Carolina University.

- Materials Specified – The materials selected for the current experimentation was limited to the use of acrylic and pure, or distilled, water due to the precedential use of both materials in the proton radiation field. The specific use of Buna-N rubber has been included in the mechanical design. All materials are considered pure in reflection to vendor claims.

- Fabrication and Equipment – The CNC equipment and tooling used to fabricate the compensator prototypes were limited to the assets of Western Carolina University and Shands Cancer Center. Purchasing customized tooling was not considered due to the excessive cost. The accuracy of the measurements are limited to the measurement devices on hand at Western Carolina University.

- Testing Sequence – The testing methods used in the current study are limited to those available to the researcher with consideration to budget and associated establishments within the field of study, such as Shands Cancer Center. The testing did not characterize the effects of the o-rings or consider the presence of

radiation scatter in the experimental design. The statistical comparisons used in the current study only investigated the means of the data.

CHAPTER 2: LITERATURE REVIEW

2.1 Background Theory

Proton therapy is a variation of particle beam therapy used to irradiate unwanted tissue. The type of unwanted tissue can range from cancerous cells to tumors; and includes both benign and malicious conditions. The key advantage of proton therapy is the ability to deliver a localized dose of radiation to a targeted area within a patient's body (Jäkel, 2009). Proton therapy's ability to deliver a localized dose of radiation is due to a phenomenon known as the Bragg peak (Jäkel, 2009).

The Bragg peak is a particular point found on the Bragg curve which is a plot of a particle's energy loss compared to the particle's depth within a given medium. As shown in *Figure 2.1*, the proton therapy makes use of the distinctive Bragg peak to target a tumor while minimizing the amount of healthy tissue exposed to the harmful radiation. As determined from *Figure 2.1*, conventional radiation therapy is recognized by a relatively high entry dose in conjunction with an easily detected exit dose. Proton radiation has the same effect on the targeted region, but has a dramatically different effect on the surrounding tissue in that the amount of radiation is minuscule in the entrance dose and almost non-existent in the exit dose (University of Florida, Proton Therapy Institute, 2009).

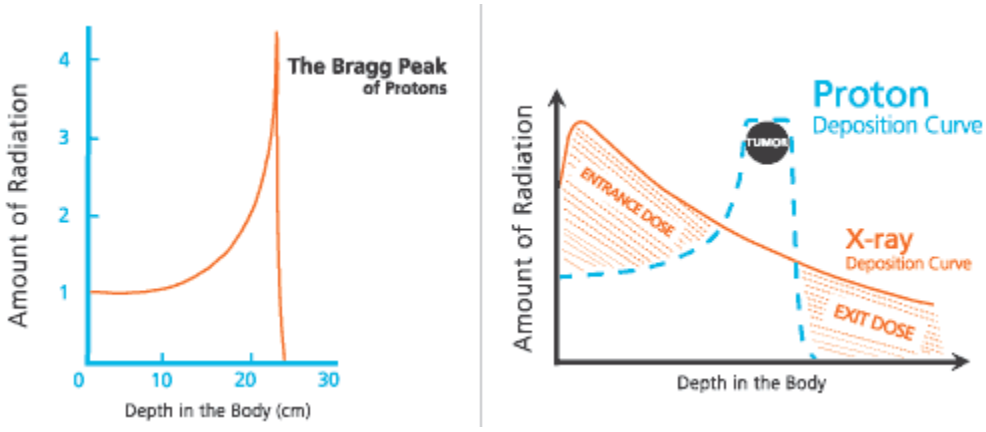

Figure 2.1: The Bragg peak (left) and a comparison tox-ray radiation (right). Online, University of Florida Proton Therapy Institute, Nov. 2009 <http://floridaproton.org>

2.2 Proton Therapy versus Alternate External Beam Therapies

Proton therapy has proven effective in treatments where the need to spare healthy tissue is urgent (Chui, 2008). Although x-ray technologies have improved their targeting capability, a recent study suggested that proton radiation therapy has a superior targeting capability (Chui, 2008). Alternative therapies, such as those who utilize photon radiation, are not capable of avoiding the irradiation of healthy tissue as shown in *Figure 2.2*. Photon radiation can be directed towards a target, but healthy tissue along the path to the target and the healthy tissue that lies beyond the target is exposed to the radiation. However, the unwanted exposure is acceptable in some situations where the benefit outweighs the harm (U.S. National Institutes of Health, 2004). Proton radiation is able to reduce the amount of radiation exposure to healthy tissue because a proton beam's speed can be controlled in such a way that allows doctors to control the point at which the radiation is released (University of Tsukuba, Proton Medical Research Center, 2007).

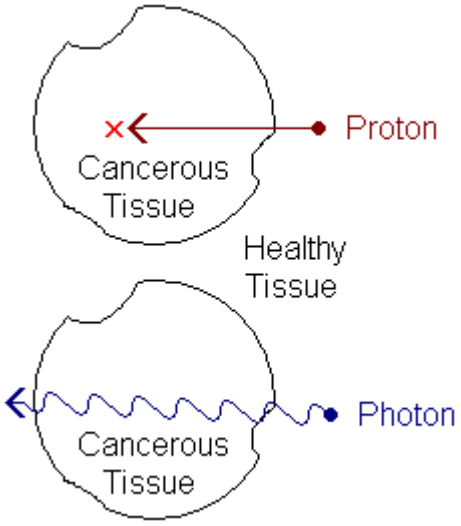

Figure 2.2: Photon radiation versus proton radiation

Some medical cases, where a patient cannot compromise the loss of healthy tissue, can only be treated with target-capable treatments such as particle radiation unless an invasive alternative treatment is possible (U.S. National Institutes of Health, 2004). According to the U.S. National Institutes of Health, doctors determine the need for more advanced treatments, such as proton therapy, by using a logical ratio commonly referred to as "the therapeutic ratio." The therapeutic ratio illustrates the amount of desired tissue damage compared to the amount of undesired damage. The radiation oncology community has conducted tests using phantom sensors to determine the precision of the various types of radiation therapy. *Figure 2.3* is a regression chart showing the dose effectiveness versus the depth within a body for photon radiation, proton radiation, and carbon radiation. The use of proton and carbon radiation has a more desirable targeting capability than the photon radiation. *Figure 2.3* also shows a Spread-Out Bragg Peak (SOBP) for proton and carbon radiation. The SOBP is the result of manipulating the radiation beam in such a way that allows the radiation to be tweaked by a depth-

compensating device (Jäkel, 2009). A compensator acts as the final beam-manipulating device that alters the radiation beam to target a specified area within a patient (University of Tsukuba, Proton Medical Research Center, 2007) as depicted in *Figure 2.4*. The use of multiple compensators allows doctors to apply particle radiation to the contours that encompass the target area. *Figure 2.5* shows a comparison of proton radiation to carbon radiation. The carbon ion has a much higher dose power and a more distinctive peak. The unwanted characteristic of heavy ion therapy is an increased amount of nuclear fragmentation; which accounts for the tail in the depth-dose distribution that extends farther beyond the Bragg peak than with proton radiation (Jäkel, 2009). The increased tail of the depth-dose distribution of particles that are heavier than protons can be seen in *Figure 2.3 and Figure 2.5*. *Figure 2.5* shows the presence of carbon radiation after the carbon ion peaks in power. The proton radiation does not have a residual down-stream effect because a proton particle can be manipulated to stop at a target. An example of the superior targeting capability of proton radiation over x-ray can be seen in *Figure 2.3*, and *Figure 2.5*.

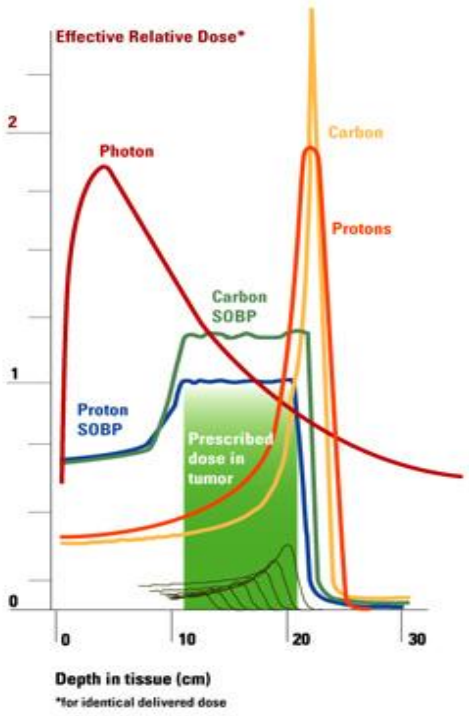

Figure 2.3: Photon radiation compared to proton radiation and carbon radiation. Online, Ion Beam Applications (IBA), Dec. 2009 <http://www.iba-protontherapy.com/benefits>

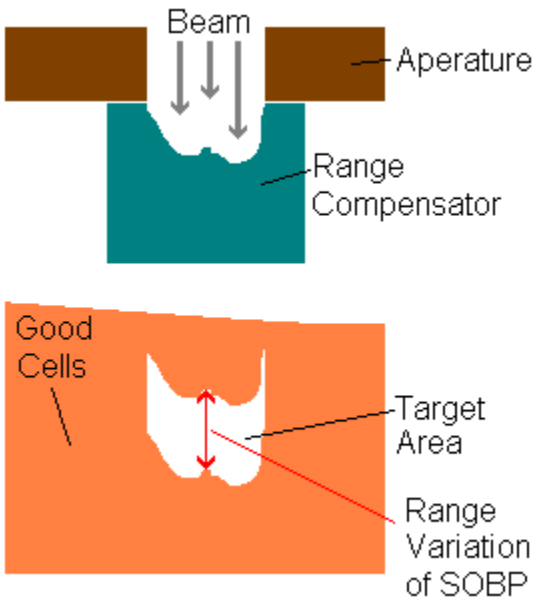

Figure 2.4: Compensator finalizing particle beam to hit a target

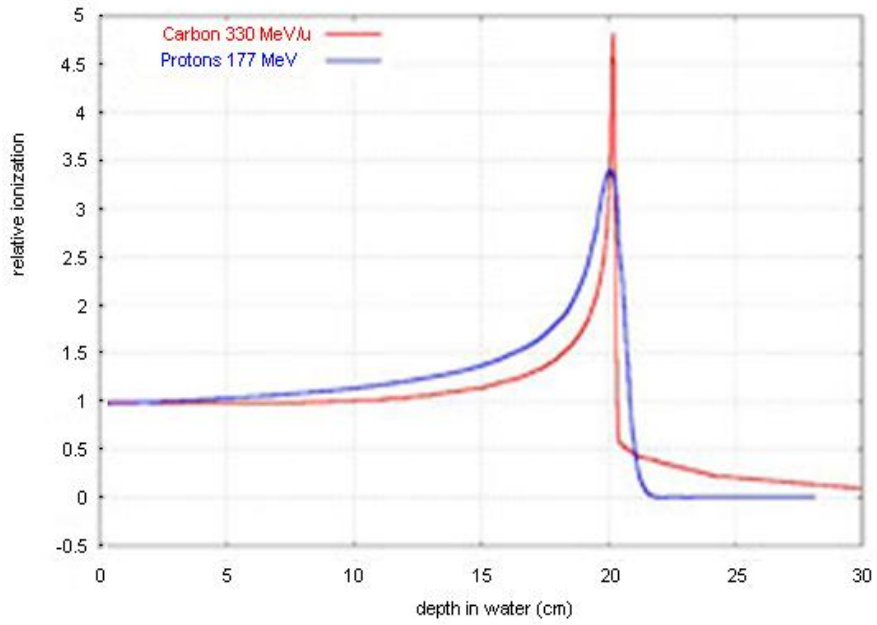

Figure 2.5: Comparison of Bragg peaks of proton and carbon radiation. Online, Advanced Cancer Therapy Foundation, Oct. 2009 <http://advanced-cancer-therapy.org/science_carbon.html>

2.3 Proton Therapy versus X-ray (Cost)

The cost comparison between proton radiation therapy and other radiation therapies such as x-ray and chemotherapy has been noted to be among proton therapy's greatest demerits (Chui, 2008). Proton radiation therapy has a notably higher cost than the conventional x-ray treatment and chemotherapy. Chui noted that the initial cost for setting up a proton radiation center ranges from $120 million to $180 million and requires an area roughly the size of a football field. According to a study conducted by Harvard medical affiliates, the cost of proton radiation therapy ranges from thirty-percent to seventy-percent more than the cost of conventional x-ray therapy (Goitein, & Jermann,

2003). Most insurance companies do not cover the cost of proton therapy unless a doctor deems the use of proton therapy critical to a patient's well being (Chui, 2008). Chui explained that special situations which require proton radiation therapy are commonly found in pediatrics and situations where the risk of irradiating a critical bodily area, such as the brain, is too high to risk. In most cases, in which conventional radiation therapy is used, the risk of damaging healthy tissue beyond a self-repairing state is acceptable (Chui, 2008). The use of radiation to treat pediatric cases require special consideration to growth hormones and physical maturity (Altman, 2004).

Working to combat the relatively high design and build costs of creating a proton therapy center, Symmetry Magazine reported that Still River Systems, a small Massachusetts company, is designing a proton therapy system that is a mere tenth of the size and cost of the current proton therapy center designs (Chui, 2008). Advances in technology suggest a more affordable price tag on proton therapy. In fact, Symmetry Magazine reported that doctors at Loma Linda center believed that proton therapy has the potential to be a cheaper alternative to conventional x-ray therapy (Chui, 2008). The principle behind the contradictory cost is due to proton radiation's Bragg peak. The Bragg peak enables a large amount of proton radiation to be delivered to a targeted area without interfering with the surrounding healthy cells. Doctors at the Loma Linda center justified that the targeting ability allows the delivery energy, or radiation, to be increased dramatically. With an increased dose, the number of sessions needed for a full treatment plan can be reduced by approximately fifty-percent (Chui, 2008). In addition to a gradual decrease in the cost of proton radiation therapy, the results of a twenty-six year study suggested that patients treated with proton radiation therapy are fifty-percent less likely to

develop secondary cancers than patients who are treated with photon radiation therapy (Loma Linda University, Medical Center, 2008). The Loma Linda Medical Center study found that 6.4 percent of proton therapy patients developed a secondary cancer while 13.1 percent, or over twice the percentage, of photon therapy patients developed secondary cancers.

2.4 Proton Therapy Center (The Overview)

Proton radiation therapy requires a complex facility capable of generating and controlling the powerful radiation beam. The proton facility at the University of Florida starts the process using H_2O. The protons are harvested from the water using electrolysis. After being collected, the protons are injected into a 444,000-pound cyclotron. The cyclotron accelerates the protons to nearly the speed of light. The protons are then directed down a pipeline that consists of a network of powerful magnets. The electromagnetic path directs the proton beam to a specific gantry system that channels the energy into a treatment room where a patient is waiting to receive the energy as shown in *Figure 2.6*. Before reaching the patient, the proton particles undergo a beam degrading device that slows the protons to a desired speed. The speed of the protons dictates the depth at which the proton will release its energy (University of Florida, Proton Therapy Institute, 2009, July).

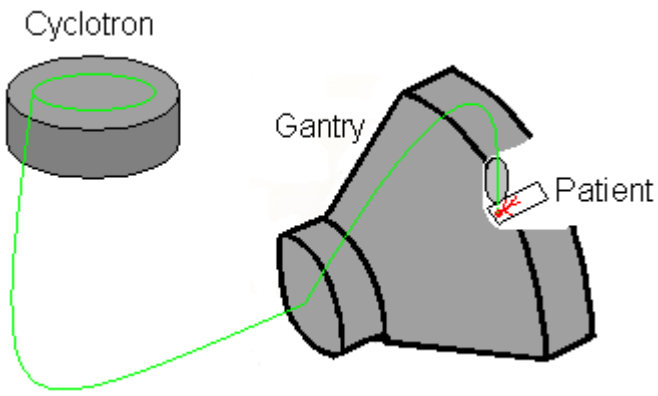

Figure 2.6: Example of proton therapy facility

2.5 Proton Therapy Process (Patient Point of View)

As is often the case with medical procedures and studies, new patients find themselves wondering what to expect through the process of the upcoming treatment. The patient process varies depending on the radiation center the patient has visited; however, numerous patients become acquainted with many of the same experiences as patients across the country. Most radiation centers make a valiant and perseverant effort to ensure the patients are comfortable at all times given the unfortunate circumstances.

For the most part, all patients experience an initial consultation visit at a radiation center. The initial consultation visit is set in place to make the patient feel comfortable with his/her doctors and the treatment center. During the consultation visit, incoming patients are given a tour of the treatment facility lasting between one and two hours in length. The tours are frequently in a more informal approach, allowing for the patients to ask questions and get individualized answers. Patients have the opportunity to view the entire facility, including many of the treatment rooms as a way to become more familiarized with the equipment and the process. After a tour, patients meet one-on-one

with his/her physician and undergo a series of questions and procedures to determine if proton therapy is the right path for the patient candidate. If preliminary tests determine that proton therapy is the best choice for the candidate, the next step in the process is to determine which type of radiation would be best suited for a patient's specific needs: proton, conventional, or brachytherapy.

The next visit that a patient would make to the proton therapy center would be for a simulation visit. During a simulation visit, physicians use x-ray images to plot the exact location of the tumor. Images are gathered using MRI-scanners, CT Scanners, and/or a Positive Emission Tomography (PET) imaging device. The precise location of the radiation area is marked out, and the physicians use the information as a means to begin the plan for the treatment process. As the first steps of the treatment plan, physicians use the gathered images of the treatment area and specialized software geared toward calculating the adequate dosage of radiation to determine the most effective course of treatment with the fewest and least severe amount of side-effects for the patient.

Once a patient begins the six to eight week treatment process, a radiation therapy facility typically keeps up with the patient's needs and interests, not just pertaining to the specific treatment of the tumor. Many facilities hold group meetings on a weekly basis for the patients. During these hour-long group meetings, patients and caregivers have the opportunity to discuss the patients' and caregivers' unique situations with other people who were experiencing, or have experienced the same treatments. The meetings allow for patients to find comfort in ongoing support provided by the facility. Some facilities even provide opportunities outside of the treatment center for patients, as is the case with the University of Florida Proton Therapy Institute. At that particular center, patients and

caregivers are provided with a weekly outing. The patients must cover his/her own expenses while on the outing, but the experience permits patients to socialize and find support with other patients in an environment outside of the specific treatment facility.

While having cancer is never found to be an enjoyable experience, the radiation treatment centers provided the patients with the best experience possible given the situation. In fact, some patients have even referred to proton radiation therapy as "a proton vacation."

2.6 Proton Therapy Process (Clinical Point of View) and How Proton Compensation Works

The initial steps for treating a patient with proton therapy includes becoming aware of the target structure within the person's body. The use of CT scans and MRI technology facilitate the radiation therapists in viewing the targeted cell structures. Using the 3D images, radiation therapists use dosimetry to derive a treatment plan for the patient's specific needs. The treatment plan often includes radiation beams being directed into a patient's body from multiple angles. The use of multiple entry angles is often necessary for maximizing the treatment of a target and minimizing the harm of healthy tissue (Massachusetts General Hospital Cancer Center, 2005).

The interaction of radiation and healthy, or unhealthy, tissue consists of the radiation particles (or "packets" in the case of photon radiation) interrupting the atoms that form the matter that tissue is made of. Once introduced to radiation, an atom's atomic structure is disrupted. The disruption consists of the tissue's atoms losing their electrons. The loss of electrons in this fashion is known as ionization. Ionization damages both healthy and unhealthy cells that are in the critical path of the radiation.

Although some radiation therapies affect healthy tissue as a casualty of treating a cancerous body of tissue, a cancer cell's ability to self-repair is typically inferior to the ability of healthy cells to rejuvenate (University of Florida, Proton Therapy Institute, 2006). Radiation oncologists use the dose-time relationship to determine the appropriate amount of radiation to use for a treatment, and the duration of the treatment (Cukier, 2004).

Proton radiation's dose distribution, as previously discussed, is characterized by the Bragg peak. The Bragg peak is generally smaller than the lesions that are commonly found on a targeted structure. Because of the Bragg peak's small size comparison, special equipment is used to combine protons of various energies to broaden, or spread out, the Bragg peak to match the thickness of a specific target. The use of multiple proton energies produces a characterization known as the Spread-Out-Bragg Peak (SOBP). Once the radiation therapists determine the dosimetry for each of the proton beam's entry angles, two components have to be designed and fabricated for each beam entry angle. The two components are known as "the aperture" and the proton range compensator, or "the compensator." Every patient has a unique condition in that their tumor's shape, size, and physical location are unique. The use of apertures and compensators allow proton therapists to adjust the particle energy to treat each patient's unique structure (Massachusetts General Hospital Cancer Center, 2005). As previously depicted, a brass aperture is created with a specific geometry that allows proton therapists to limit the proton beam to the 2D outline of the target. The proton beam passes through the opening in the aperture and enters the proton compensator. The proton compensator adjusts the range of the proton beam to match the topography of the target within a

patient's body. The proton beam passes through the range compensator where the proton is actually slowed down. After traveling through the compensator and any healthy tissue that may lie between the surface of the patient's skin and the targeted area, the proton is slowed to a point that its full energy is exposed to the targeted area (The National Association for Proton Therapy, 2009). The increase in energy emitted from the proton is due to the fact that the proton is slowing down and stopping at a specified depth. Protons slow down as they pass through matter. The density of the matter dictates the rate of how much a proton is slowed down. The heavier the matter, the greater the impact on the proton's speed (Massachusetts General Hospital Cancer Center, Department of Radiation Oncology, Harvard Medical School, 2005).

As a proton moves through a mass, the energy contained is lost because of the interaction of orbiting electrons. Because the proton slows as it travels through the compensator, proton therapists adjust the compensator to make sure that the proton slows and stops at a targeted point within a patient (The National Association for Proton Therapy, 2009). The use of apertures and compensators are the key to minimizing radiation exposure to healthy tissue.

After the fabrication of custom apertures and range compensators has been completed, proton therapists prepare patients for treatment. The main objective in the treatment procedure is to constrain the patient in a stationary position so the radiation beam will hit the intended target. The methods for constraining the patient range from a partial brace to a full-body restraint depending on the location of the target. Once constrained, radiation therapists compare x-rays, which were taken before the treatment, to an image from the treatment-planning CT. The image comparison process ensures that

the patient is properly aligned with the proton gantry system (R. Helmig, personal communication, May, 2009).

In most cases, patients undergo multiple sessions of proton radiation therapy. Some patients only have to undergo one or two proton therapy sessions. Shorter terms are usually applicable where patients have lesions that are contained within the head and require the treatment known as Proton Stereotactic Radiosurgery (PSRS). PSRS sessions are usually about an hour in duration and can be completed in one or two sessions (Massachusetts General Hospital Cancer Center, Department of Radiation Oncology, Harvard Medical School, 2005). Proton Ocular Radiotherapy (PORT) is a treatment that addresses ocular lesions that are contained within the human eye. PORT sessions are approximately ten-to-twenty minutes in duration and can be delivered in two-to-five sessions (Massachusetts General Hospital Cancer Center, Department of Radiation Oncology, Harvard Medical School, 2005). One of the longer types of proton radiation therapy is Proton Stereotactic Radiotherapy (PSRT). PSRT involves the treatment of lesions throughout the entire body. PSRT sessions typically take twenty-to-forty minutes to complete, and there can be as few as five or as many as forty sessions needed to properly treat a patient's condition (Massachusetts General Hospital Cancer Center, Department of Radiation Oncology, Harvard Medical School, 2005).

2.7 Fabrication of Apertures

Proton beam apertures are responsible for shaping the proton beam to the outline of the targeted area within a patient. The aperture is typically made from brass in a machine shop. A Computer Numerical Controlled (CNC) mill is programmed to cut the specific profile in accordance to the proton therapists' specifications. The apertures are

typically designed to be one solid object, but sometimes machinists make the larger compensators in layers so that technicians can mount the apertures in the proton equipment easier (Bates, 2006).

2.8 Fabrication of Range Compensators

The current procedure for creating a custom radiation compensator requires doctors to outsource to a machine shop unless a CNC machine shop is available in-house. The process of making proton compensators starts with a three dimensional (3D) computer model used to generate CNC code for a milling machine to decipher. Once the CNC code is generated, a machinist prepares a blank proton compensator for milling. The blank proton compensator consists of an acrylic block that is typically pre-cut to fit into the proton gantry system. Proprietary software packages have been created to bypass the need for machine operators to use a 3D model to create CNC machine code. The University of Florida's Proton Therapy Institute uses a customized software package that generates machine code directly from the dosage values generated by dosimetry calculations (R. Helmig, personal communication, April, 2009). Smaller compensators, such as those used for prostate cancer patients, can typically be fabricated in 35-75 minutes (R. Helmig, personal communication, April, 2009). Other compensators, especially for cases that involve the treatment of large tumors, may require several hours of machining (Bates, 2006). Outsourcing the fabrication of range compensators may take up to several days to be fabricated and delivered.

2.9 Testing Effectiveness of Proton Range Compensators

Radiation therapists perform quality checks to verify the proton equipment is operating as intended. Although a multitude of sensors monitor a cyclotron and gantry

system, a actual simulation test is used to check whether the proton energy is hitting the intended target or if the integrity of the beam is being lost (Jäkel, 2009). The test consists of the compensators being placed in the path of a proton radiation beam. A proton radiation beam will pass through the compensator and into a plastic phantom. The plastic phantom is a device that acts as the recipient of the treatment. The phantom is armed with a 2-D detection device that will detect the radiation dose, at multiple levels within the phantom, and at multiple energy levels. According to Siyong Kim, a proton radiation expert at the University of Florida's Proton Therapy Institute, the detection devices are basically a film that has a high spatial resolution (K. Siyong, personal communication, Dec. 17, 2009). The images that are imbedded into the film are then processed and assign an Optical Density (OD) that can be used to determine the dose created. The OD is converted into dose using an established OD-to-dose conversion curve. The data gathered during the test is recorded into a 2-D matrix of numbers (K. Siyong, personal communication, Sept. 22, 2009). An example of a phantom device with a solitary sensor is shown in *Figure 2.7*.

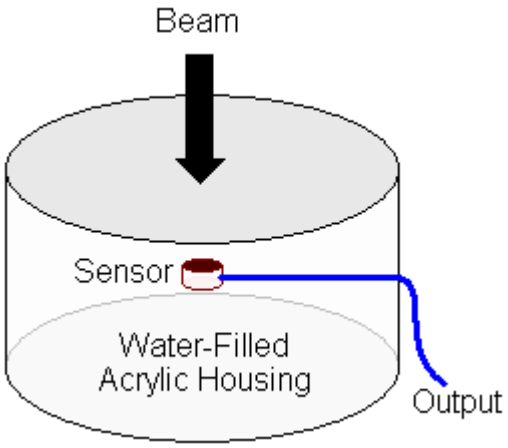

Figure 2.7: Example of phantom sensor

The current operational procedure for determining the absorbed dose-to-water in all operating ion facilities is based on ionization chamber dosimetry (International Atomic Energy Agency, 2000). Due to the current procedure for calibration, commercial ionization chambers are used. Commercial ionization chambers are calibrated by the Secondary Standard Dosimetry Laboratory (SSDL) in a field of Co-60 in terms of absorbed dose-to-water (Jäkel, 2009).

Although the use of the SSDL is common for initial calibration testing, the use of water phantoms and films are commonly used for dose verifications and routine quality checks. The use of solid state detectors, such as film, in ion beam dosimetry can be problematic due to a quenching-effect within a signal in areas with increased linear energy transfer (Jäkel, 2009). Despite the undesired effect associated with ion dosimetry, the use of film exposures in routine quality checks is acceptable. The use of film in proton dosimetry is acceptable because the effect of linear energy transfer can be accounted for as a function of depth (Jäkel, 2009).

CHAPTER 3: METHODOLOGY

3.1 Preliminary Procedures & Material Selection

Prior to the design and fabrication of the fluid-based compensator prototypes, a logical review of available materials and fabrication processes was conducted. The first constraint set was governed by the availability and acceptability of materials for use in proton radiation therapy. The major concern for material acceptability was based off of a concern for radiation scattering when passed through materials with a high-Z value. For the purpose of finding acceptable materials, a "rule of thumb" was established by Dr. Phillip Sanger, the director at The Center for Rapid Product Realization, at Western Carolina University, for eliminating potential high-Z materials. The basic approach using the "rule of thumb" was to avoid using materials with atomic elements, found on the periodic table of elements, below the second row. In general, the periodic table of elements has relatively lower-Z materials on the top row; and higher-Z materials on the bottom row (Mozumder, 1999).

A search for a suitable OEM product that could suffice as primary housing for multiple fluid chambers produced no acceptable candidates. Hexagonal arrays, and basic round arrays, were sought after. Potential OEM products were found; but, each lacked the mechanical criteria necessary (material composition, thickness/length of chambers, structural consistency, and structural integrity). The consensus from potential manufacturers suggested that the parts could be custom-made to allow for a mass production of a hexagonal array, but the "custom" nature of the product extended beyond the financial feasibility of this study. A conclusion was made that focused efforts to make the primary housing completely from scratch. Acrylic, or "Lucite," was selected as

the medium of choice due to availability and precedent use in proton radiation compensators. A 3D constraint-based solid model of the main housing can be seen in *Figure 3.1*.

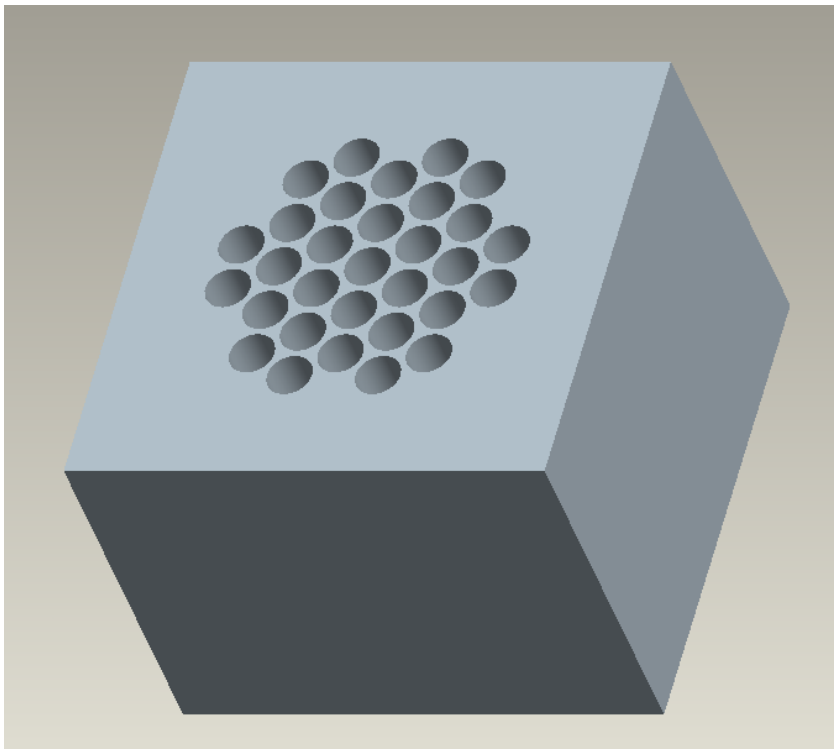

Figure 3.1: Compensator main housing

Manipulating the fluid levels to conform to a dosimetric prescription was expected to be regulated by a physical plug to ensure the fluid did not move inside of the chambers due to the capillary effect. The search for an OEM product to serve as a plunger yielded problems because the physical shapes and sizes did not conform to the current design. The plugs could have been made custom, but tooling would be too costly. The plugs were made in-house at Western Carolina University (WCU). Although WCU has the capability to injection mold parts, the time and effort associated with setting

WCU's equipment up for the molding process would have been out of the scope of the study. The plug had to be designed to be made using subtractive machining technology capable of being performed with WCU's CNC equipment. A 3D constraint-based model of the plug can be seen in *Figure 3.2.*

Figure 3.2: Acrylic plug with o-rings

The fluid-based compensator required a decision to be made concerning the type of fluid to be used in the experimentation. A low-Z material was necessary to fill this role. The initial fluids considered included water (H_2O), glycerin [$C_3H_5(OH)_3$], and sucrose ($C_{12}H_{22}O_{11}$). Distilled water was selected because of precedential use in oncology (R. Helmig, personal communication, September, 2009).

The fabrication stage of the current study was limited to the equipment and tooling that was readily available to the primary researcher due to scheduling constraints. The length of flat-ended tool necessary to cut the deep chambers for the prototype had to be custom made. Although specialty tooling can be custom made for cutting plastic

material, the cost was avoided by ordering an OEM tool. The tool used for cutting the chambers was a .375-inch-diameter, titanium-nickel coated, four-fluted end-mill with a 3 -inch-of-cut capability. A custom-made tool would have left a better surface finish, but for the purposes of this study, the tool selected was adequate for enduring the defined conventional CNC tooling paths.

3.2 Prototype Design & Assembly

The conceptual design of the fluid-based range compensator was developed based on the current fabrication capability of this study. Based upon the constraints discussed in the previous section, a circular array was developed to house water. The fluid level would be controlled by a network of custom-made acrylic plugs with Buna-N o-rings. The o-rings were an OEM product that had a square-shaped cross-section. The principle behind the square cross section was to make the design as uniform as possible, in terms of depth, so that obscure results could not be dismissed as an effect of radiation passing through un-uniform, or rounded, surfaces. The prototype was designed to be assembled in a water bath. The reason for submerging the parts while assembling was to avoid air bubbles from getting into the chambers while inserting the plug. Once assembled, the plugs were pressed to a desired depth using a pre-cut push-off tool. The push-off tool was custom made, to a tolerance of +/- .001 inches to press the plugs down to a pre-determined depth. When the plugs were depressed, the displaced fluid passes through a small weep-hole in the bottom of the chamber as shown in *Figure 3.3*. The diameter of each column was designed to be .3750 inches +/- .002 inches in diameter; with a weep-hole of .0280 inches +.001 inches / -.000 inches in diameter. The reason for the small

weep-hole was to allow water to pass through when a plug is depressed, but not when the plug is set to an intended depth.

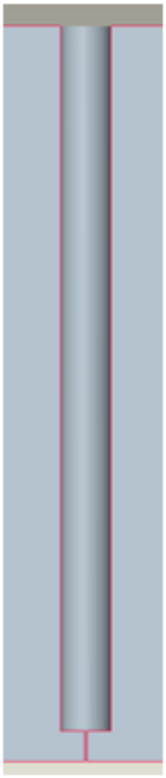

Figure 3.3: Cross-section view of fluid chamber with weep hole

3.3 Fabrication Procedure

The fabrication procedure used to create the fluid-based compensator prototypes required attention to detail to ensure that each part was created uniformly. In order to verify that the parts were as uniform as possible, the same tooling setup was used for each of the specimens created. The CNC equipment was checked to ensure that their positional coordinate system was justified to the same location during the mill and lathe operations. The cooling method used to ensure the tooling, and acrylic, did not overheat

during the machining process relied on the combination of medium-viscosity mineral oil and air pressure.

Starting at the beginning of the process for creating the main housings for the compensators, acrylic stock was received and surface-milled to the outer dimensions needed. Each block was machined in the same machine using the same offset coordinates. The blocks were then positioned within a mill to begin the tooling operation that creates the holes in which the fluid would be held. This operation consisted of a drill bit performing a peck-drilling cycle to pre-drill the holes. After the pre-drilling cycle was complete, an end-mill performed a peck-drilling operation to finish the holes. The original intention of this tooling operation was to follow the end-mill cycle with a reaming operation. But, due to an unexpected gyration of the end-mill, the holes were too wide for the reaming operation to be effective. The holes were checked for consistency using a calibrated coordinate measuring machine. All of the holes proved to be consistent and smooth enough to continue the fabrication process without the need to restart the process. Although the surface finish was not ideal, the purpose of this study did not hinge upon the perfection of the surface finish; the focus of the current study was to analyze the feasibility and effectiveness of the prototype's conceptual design.

Once the main fluid chambers were finished, the acrylic block was flipped upside-down to begin the creation of the weep-holes. A small carbide drill bit, .0280 inches in diameter was used for a peck-drilling operation. The mechanical capability of the small drill bit required extra attention to ensure the tool did not break off into the acrylic block. The weep-holes could have been made prior to the main fluid chambers; but would be prone to have resulted in the small holes becoming clogged from the presence of the

waste material that would be removed in the tooling cycle associated with the fluid chambers.

The accuracy of each of the depths was maintained to be +/- .001 inches of the intended values. The depth of the uniform depth specimens was 1.000 inches and the multi-depth specimens had three different levels. The three levels were 2.000 inches deep, 1.250 inches deep, and .250 inches deep. All depths were checked multiple times using calipers that were accurate to +/- .0005 inches.

3.4 Photon Radiation used to Test Proton Range Compensator

The use of proton particle radiation is the preferred choice for testing the effectiveness of an experimental proton range compensator. However, due to logistical constraints, and a limited funding for the early stages of the current study, the use of proton radiation testing will not be used for this study. Instead of using proton radiation to verify of the proton range compensators, the use of photon radiation will be used as a comparable alternative. The substitution of photon radiation for proton particle radiation, for use in the current study, has been verified by radiation experts at Shands Cancer Center (R. Helmig, personal communication, January, 2010). Dr. Chihray Liu, the chief of physics at Shands Cancer Center, explained that the use of photon radiation to compare the proposed compensator to the existing compensator was adequate to check the general effect of the compensator design (Dr. C. Liu, personal communication, March, 2010). Proton therapy and photon radiation therapy are both capable of being manipulated by introducing a medium of choice within the radiation's path (Attix, 2004). Protons and electrons both undergo angular scattering during their projections into a

medium. However, the use of photon particle radiation yields a smaller average for the scattering angles due to the superior ballistic properties of protons (Jäkel, 2009).

3.5 Experimental Design

The goal of the current research was to determine the feasibility of using a fluid-filled proton radiation compensator design in comparison to the existing design through the implementation of a real-world test. An existing proton compensator (control) was analyzed and compared to a fluid-based compensator prototype. The experimentation portion of the project included the design and fabrication a fluid-based particle compensator that was tested at SHANDS medical research center at the University of Florida's Radiation Oncology Department. The fluid-based compensator design was compared to the conventional proton compensator design through a real-world testing sequence. The test consisted of the compensators being placed in the path of a photon radiation beam. The photon beam passed through the compensator and into an electronic detection device. The detection device served as the recipient of the treatment. According to Bo Lu M.S., instructor in radiation oncology at Shands, the detection device consisted of a 2-D array of sensors that acted as a film exposure when exposed to a light source. The detection devices were basically an electronic form of a film that has a high spatial resolution. The images that were detected via the detection device could then be processed and assigned an optical density (OD) used to determine the dose created. The OD can be converted into dose using an established OD-to-dose conversion curve; but, for the intent and purpose of the current experiment, the data was processed using MATLAB® software and assigned a grayscale value for each pixel of the exposure

images. The process of using the grayscale values, instead of the OD curve, to compare the data sets was justified by Chihray Liu, PH.D., the chief of physics at the University of Florida's radiation oncology department, because the grayscale-approach was adequate for the comparison and would simplify the data processing for the current study. The data gathered during the test was recorded into a 2-D matrix of numbers. The matrices from the two testing sequences were compared to determine the feasibility of the fluid-based design in comparison to the conventional compensator design. The matrices of dose values detected were compared to determine the statistical difference between the compensators.

The nature of the current study could benefit from an understanding of the impact of multiple aspects of a fluid-based compensator design versus a conventional solid design. *Figure 3.4* represents five different configurations for the range compensators. All five configurations are shown on the same block of material for comparison reasons only; the compensators were separate units. The compensator configurations were as follows: starting at the top left of *Figure 3.4*, fluid-based with plugs set at one depth (top left); solid design with webbing present cut to a uniform depth (top middle); and solid design without webbing cut to a uniform depth (top right); fluid-based with plugs set at multiple depths (bottom left); and a conventional design that represents an existing compensator design (bottom right). The depths of the top row of configurations are all the same depth. The two multi-depth configurations will be adjusted to be the same configuration. The various different designs could be used to determine the impact of the fluid, the presence of the webbing between columns, and the effect of having multiple depths with fluid.

Compensator/ Specimen #	Key Physical Characteristics
1	Fluid-based design adjusted to a 1" uniform depth
2	Solid-based design fabricated to be at a 1" uniform depth; includes a web-like structure to replicate compensator 1
3	Solid-based design fabricated at a 1" uniform depth
4	Fluid-based design adjusted to three different depths
5	Solid-based design adjusted to three different depths to physically match depths of compensator 4

Figure 3.4: Specimen identification

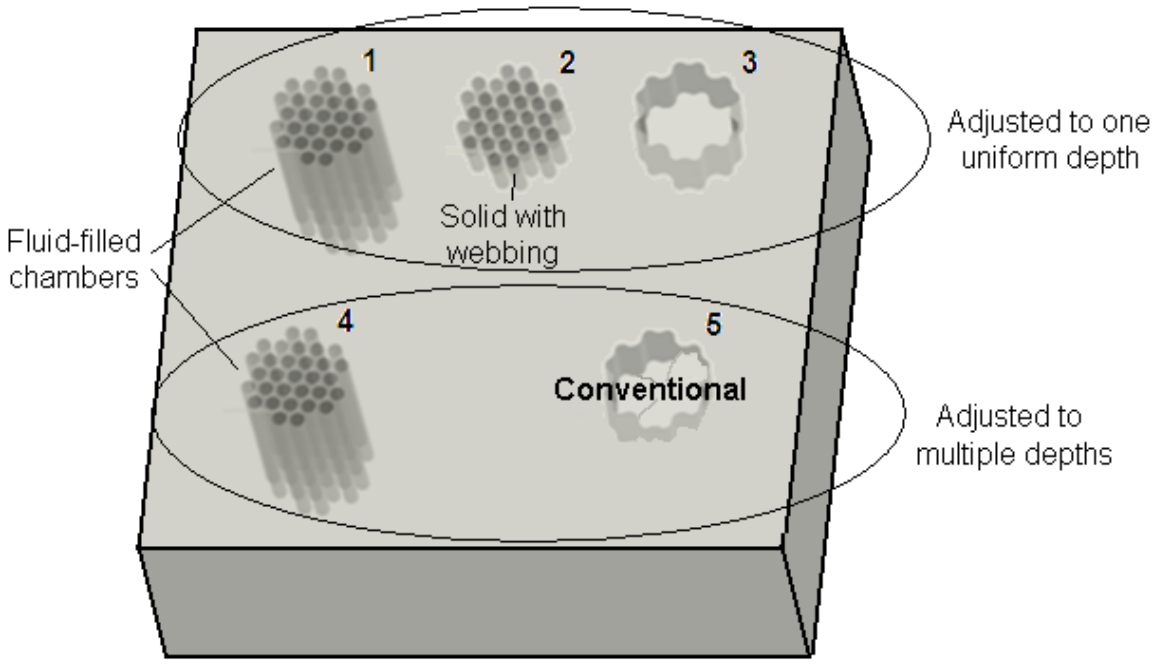

Figure 3.5: A visual rendering of the five compensators compared

3.6 Experimental Procedure

The experimental procedure used in the current study consisted of placing each of the five compensators, individually, in the path of photon radiation as shown in *Figure 3.6*. Each of the specimens was visually aligned to be at the center of the radiation field. The intent was to have the compensators positioned at the exact same location; but, at the time of testing, the best method for alignment was based off of a shadow alignment procedure that consisted of using personal judgment to center each specimen within a box as shown in *Figure 3.7*. The shadow of the compensator was the result of a light source, located in the radiation source that emits light to show the outlining shadow of the compensator. Once aligned, Bo Lu M.S., a trained radiation oncologist at Shands radiation oncology center, aided in the irradiation of each of the specimens. The results of a radiation session, such as those in the current study, could be analyzed by converting the values to a numeric value and to a pre-established dose-deposition curve. But, for the intents and purposes of the current study, the results were saved as an image, and converted to a matrix of grayscale values. More specifically, the results of each of the five compensators were saved in the form of a tag image file format (.tif). The tiff files were then entered into the MATLAB® software package and pixilated. Each pixel had a grayscale value ranging from 0-to-255, or black-to-white. The grayscale values were converted to individual matrices. Each matrix corresponded to a particular specimen.

Figure 3.6: Compensator testing setup

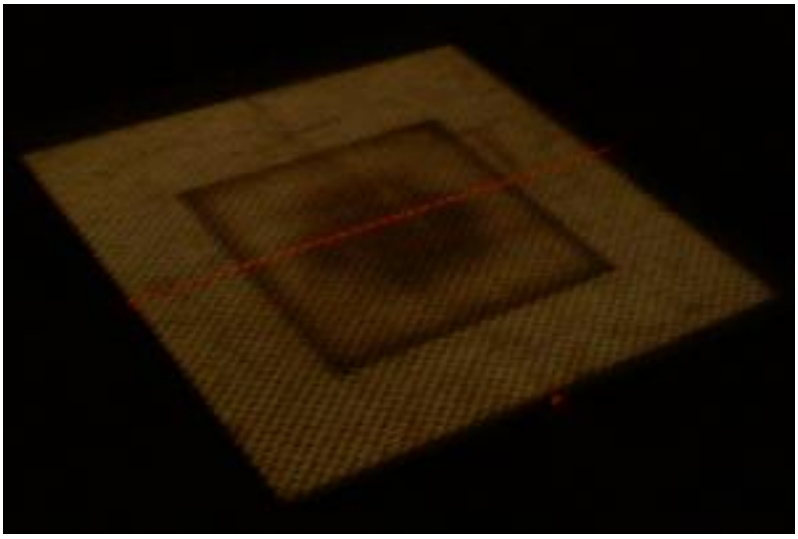

Figure 3.7: Compensator alignment for testing

Prior to transforming the .tif images to five separate matrices, the images were aligned. The original intent during the testing sequence was to have a mounting mechanism available to align the specimens. Due to unforeseen events, the precise mounting mechanism was not available at the time of the testing. In order to compensate for the lack of precise alignment, the images were cropped and rotated to visually align the images. The initial .tif images can be seen in *Figure 3.8*; the aligned and cropped tiff images can be seen in *Figure 3.9*. Once aligned, the matrices could be compared using paired t-tests on a pixel-to-pixel basis.

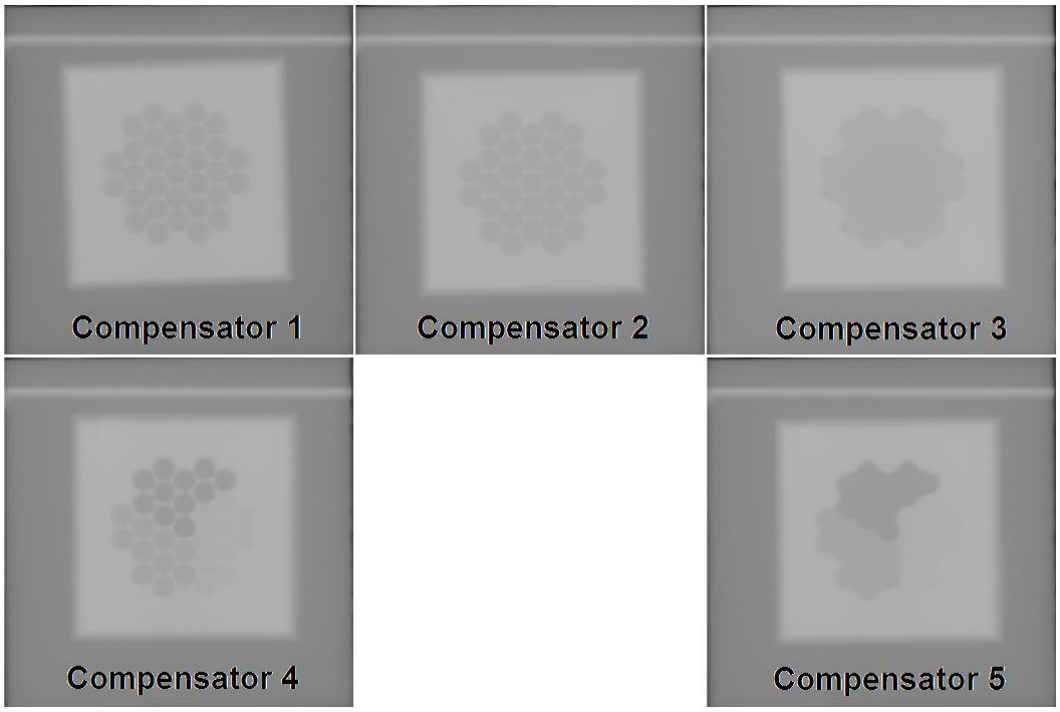

Figure 3.8: Original .tif images

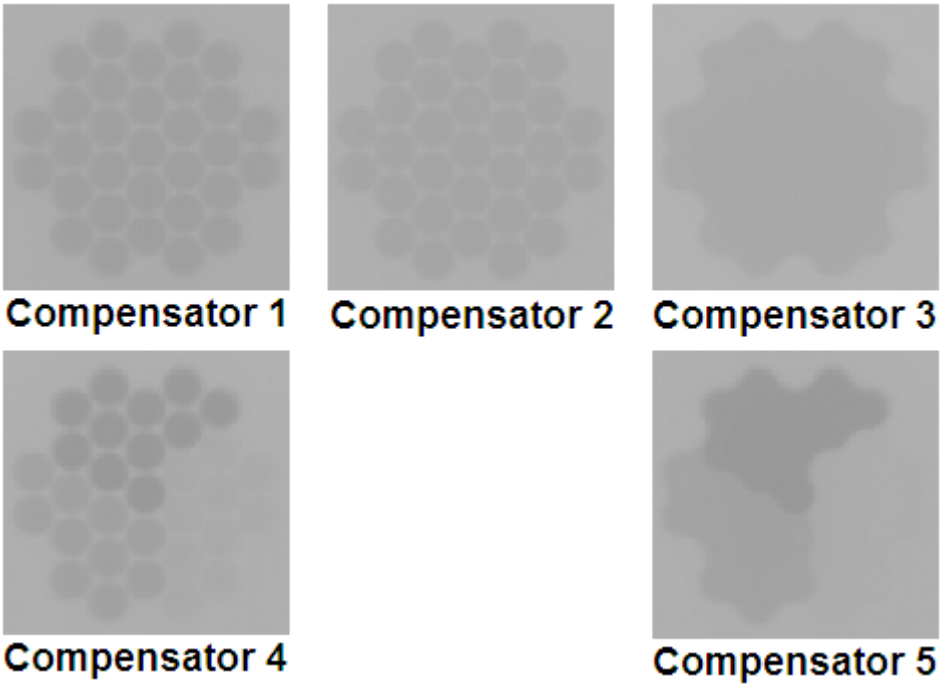

Figure 3.9: Aligned .tif images

3.7 Measurement Method

The results of a radiation session, such as those in the current study, could be analyzed by converting the values to a numeric value and to a pre-established dose-deposition curve. But, for the intents and purposes of the current study, the results were saved as an image, and converted to a matrix of grayscale values. More specifically, the results of each of the five compensators were saved in the form of a Tag Image File Format (tiff). The tiff files were then entered into the MATLAB® software package and pixilated. Each pixel had a grayscale value ranging from 0-to-255, or black-to-white. The grayscale values were converted to individual matrices. Each matrix corresponded to a particular specimen. After rotating and cropping the tiff image, as shown in *Figure 3.9*, the matrices of numbers were 460 x 460 grayscale pixel values in size.

3.8 Procedure for Analyzing Data

The inferential used in the current analysis included a combination of an analysis of variance (ANOVA) and a paired-t-test. T-tests were used to apply an inferential value to the differences between the three specimens adjusted to a uniform depth illustrated in the top three configurations of *Figure 3.5*. The t-tests provided a p-value to determine the statistical differences in the fluid-based design and the solid/conventional design. Also, the t-tests applied a p-value to determine the overall effect of having webbing between the columns (referring to the material that separates the holes). A paired t-test was used to compare the fluid-based, multi-level, specimen to the conventional, multi-level, specimen as depicted on the bottom row of specimens shown in *Figure 3.5*. *Figure 3.10* shows a close up of the individual points that were referenced for the analysis. The numbered points shown in *Figure 3.10* were paired with the coinciding points in the conventional compensator design for the statistical analysis. P-values were used to express the statistical difference between the paired points. Each point refers to the location of each of the thirty-one individual holes, or locations, on each of the five compensators.

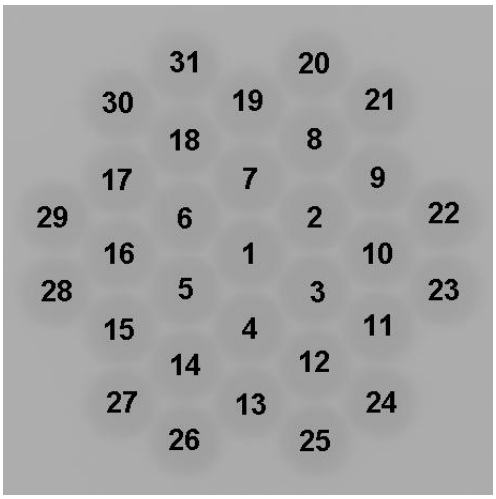

Figure 3.10: An illustration of the individual holes/points on the fluid-based design

The current analysis also makes use of descriptive results to add more detail to the inferential results. Both, inferential and descriptive results should be studied because each will contribute aspects to the understanding of the data (Box, 2005). Box explains the inferential statistic analysis verifies if a given set of data is numerically the same in accordance the parameters of a specific test; and the descriptive results can visualize aspects of a set of data that are not represented in the inferential results.

3.9 Analysis of Variance (ANOVA)

An ANOVA's purpose is to determine if there are statistical differences in the mean values of data sets (Schiff, 1996). For the current study, a null hypothesis that was used specified that the means of compensators 1, 2, and 3are the same; and compensators 4 and 5 have the same means. The null hypothesis was:

$$H_0: \mu_{COMPENSATOR1} = \mu_{COMPENSATOR2} = \mu_{COMPENSATOR3}$$
And
$$\mu_{COMPENSATOR4} = \mu_{COMPENSATOR5}$$

The alternative hypothesis was specified that not all, or not any, of the compensators would have the same mean. The alternative hypothesis was:

$$H_A: \mu_{COMPENSATOR1} \neq \mu_{COMPENSATOR2} \neq \mu_{COMPENSATOR3}$$
And
$$\mu_{COMPENSATOR4} \neq \mu_{COMPENSATOR5}$$
… Any variation indicating that all means are not equal

After running an ANOVA to analyze the differences between compensators 1, 2, and 3, a t-test was used to analyze the differences between compensators 4 and 5. A paired t-test analysis is used in situations where two sets of data requires a comparison that considers that each data point should be compared to a corresponding data point in the opposing set of data (Box, 2005). Box explains, before using an ANOVA, certain assumptions have to be met to properly use the analysis. Box continues, in order to run an ANOVA, the data must be normally distributed; and the variances should be equal. In the event that the variances are not equal, a two-sample t-test should be used to properly analyze the data (Box, 2005).

CHAPTER 4: ANALYSIS AND RESULTS

4.1 Data Summary

The data used to compare the compensator specimens were extracted from the photon radiation scans, in the form of .tif images, and transformed into a numeric value to be analyzed statistically. The .tif images were rotated visually and aligned using human judgment to compensate for variability in the testing apparatus as discussed in *Chapter 3****Error! Reference source not found.***. Once aligned, each .tif image was converted to a 2D matrix of grayscale values. The grayscale values were extracted from the image, pixel-by-pixel, to create a 460 x 460 matrix for each of the five compensator specimens.

4.2 Inferential Statistics

Upon the first iterations of the statistical tests, a paired t-test was used to determine the similarity in the means of specimens 1 and 2. Again, specimen 1 was the fluid-based design adjusted to one uniform level; and specimen 2 was a solid version, adjusted to the same level with webbing included to equalize the comparison. The statistical analysis of the paired t-test produced a p-value below .05, operating under a 95-percent confidence interval. The p-value, as shown in *Figure 4.1*, was 0.000 which indicated that, , specimen 1 was statistically different than specimen 2. Similar paired t-tests were run concerning the differences between compensators 1 and 3, 2 and 3, and 4 and 5. The results of the other un-adjusted paired t-tests can be found in *Appendix D*. The multiple paired t-tests resulted in p-values below .05; suggesting that the raw grayscale data recorded was statistically different.

```
Paired T for Specimen1 - Specimen2
                 N      Mean    StDev  SE Mean
Specimen1   211600   166.670    5.244    0.011
Specimen2   211600   170.663    4.373    0.010
Difference  211600  -3.99233  1.18939  0.00259

95% CI for mean difference: (-3.99740, -3.98726)
T-Test of mean difference = 0 (vs not = 0):
T-Value = -1544.04  P-Value = 0.000
```

Figure 4.1: Paired t-test for specimens 1 and 2 – unadjusted

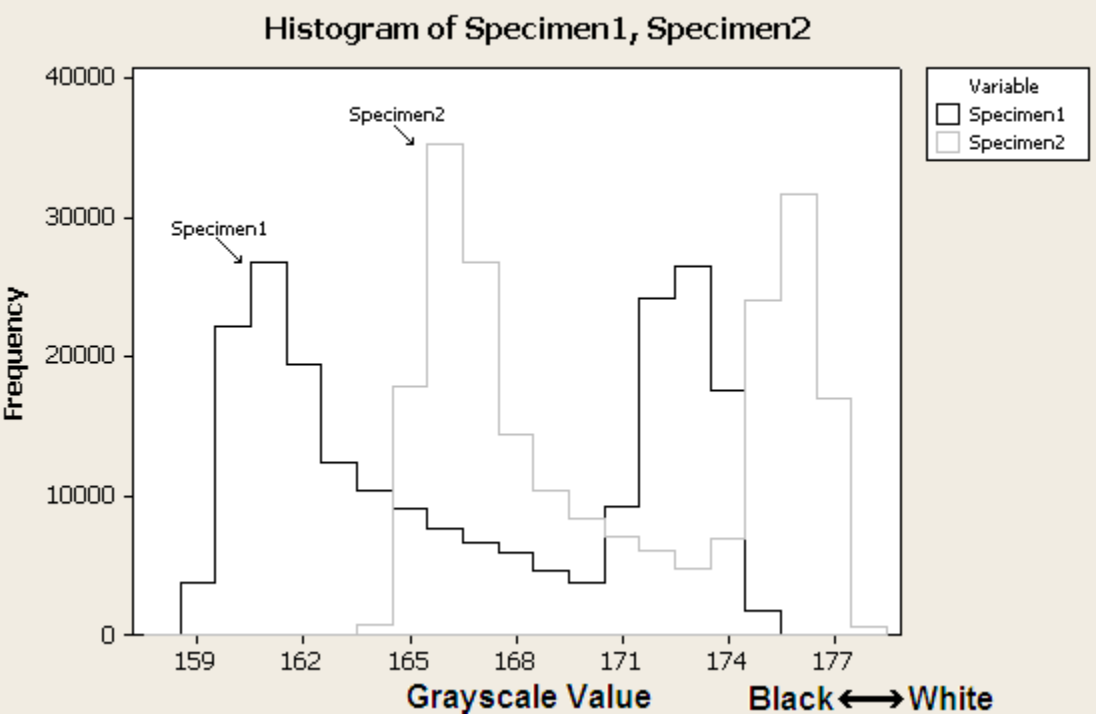

Figure 4.2: Histogram of specimens 1 and 2 – unadjusted

4.3 Adjusting Data

The need for adjusting the data was apparent upon comparing regions of the .tif images that should have been uniform due to the identical physical traits. The use of descriptive statistics was used to identify aspects of the data that needed to be

normalized. Photon radiation has been known to deviate from a nominal value; which may explain the need to use means to calculate dosimetric values (Attix, 2004). Furthermore, Professor Frank Attix explains that a common practice used to estimate the accuracy of radiation is to determine the standard deviation of a given dose. The image shown in *Figure 4.3* references a common region on each of the five compensators that consists of a 30x30 pixel area. The grayscale values within the defined areas were averaged; and the differences in these means were compared. The differences in the mean values suggested the photon radiation was not entirely consistent for each of the five compensator tests. According to Frank Attix, a slight fluctuation in a radiation beam is normal; and an average dosimetric value is taken to quantify a uniform dose (Attix, 2004). The likelihood that the variance of intensity was due to inconsistency within the acrylic material was very low. In an effort to compensate for the normal fluctuation in the photon radiation beam, the grayscale values of each compensator were shifted by the calculated differences in the means. The new adjusted values were compared using paired t-tests and ANOVAs to analyze the differences in the mean values of the newly adjusted matrices. As shown in *Appendix E*, the efforts for normalizing the data produced no change in the p-value, which remained below .05 (p-value remained 0.000 for each comparison) regardless of the specified normalization points.

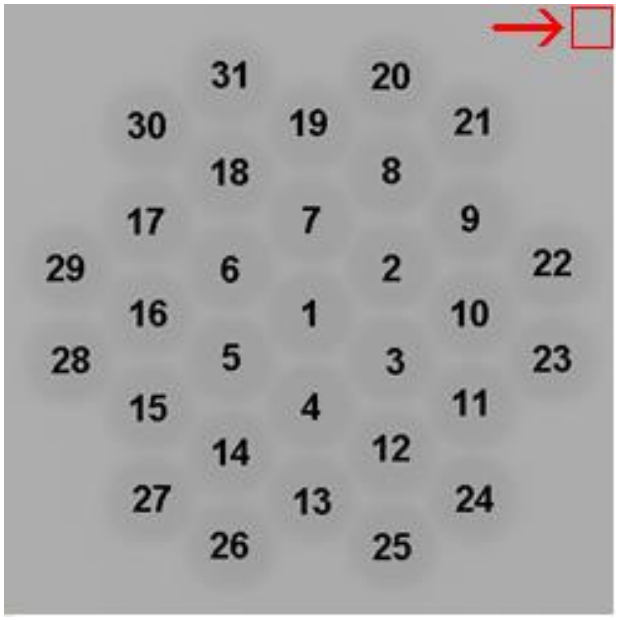

Figure 4.3: Common section in specimens

Similarities in the appearance of the results shown in *Figure 4.4*, and the enhanced view of beam fluctuation in *Figure 4.5* were noticeable due to the amount of variance in intensity from test-to-test, and within a single exposure. For example, the upper right compensator shown in *Figure 4.5* was a solid acrylic block with a pocketed area that was characterized by a smooth, even surface. Through visual enhancement, the image shown in *Figure 4.5* suggests that there may be a variation of intensity ("hot spot") within the radiation field. The scatter plot shown in *Figure 4.6* illustrates a noticeable fluctuation in the radiation intensity across a single compensator; which is characterized by a slanted distribution of data that should be level (horizontal distribution). The use of a paired t-test, or an ANOVA with blocking applied should compensate for the inconsistencies. However, the locations of the inconsistencies were shifted when the raw images were cropped and rotated to be aligned properly. In order to truly measure the

differences, through the use of blocking variables, the alignment of the structural features and the “hot spots” are required.

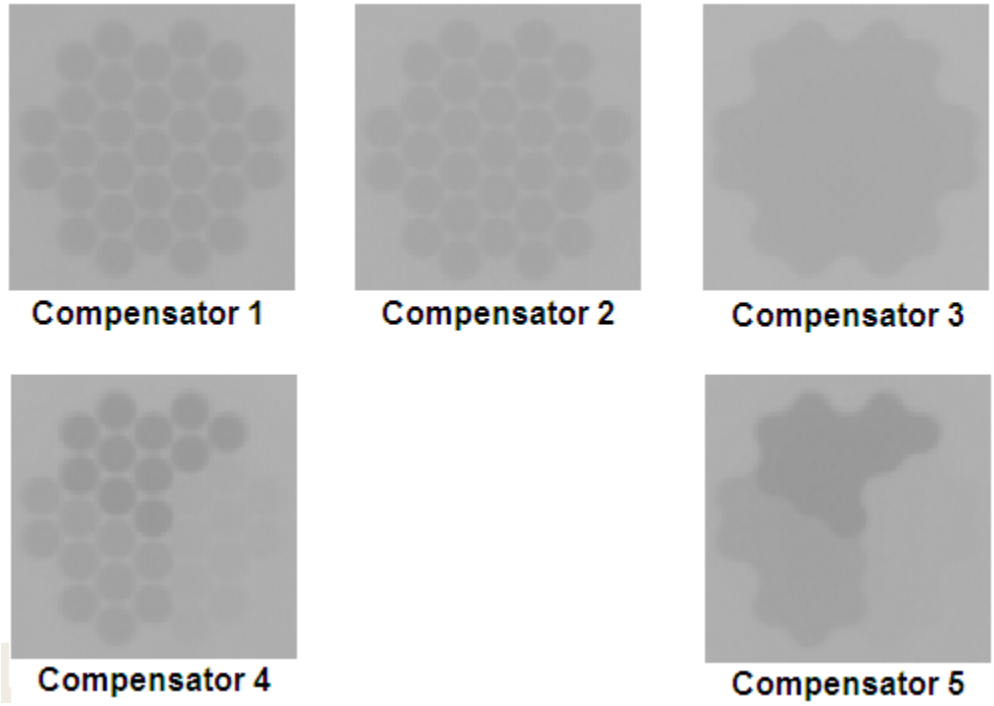

Figure 4.4: Aligned .tif images

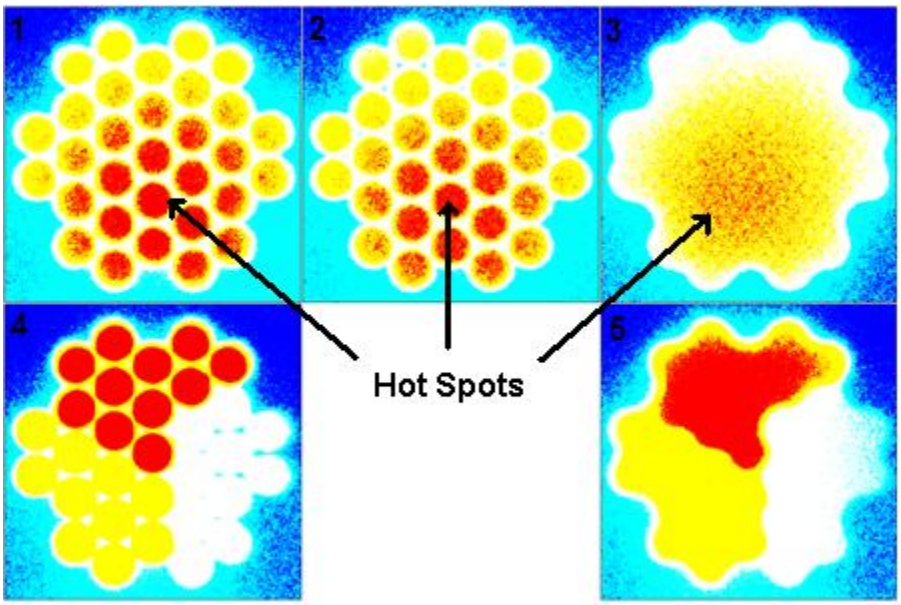

Figure 4.5: Aligned and enhanced .tif images

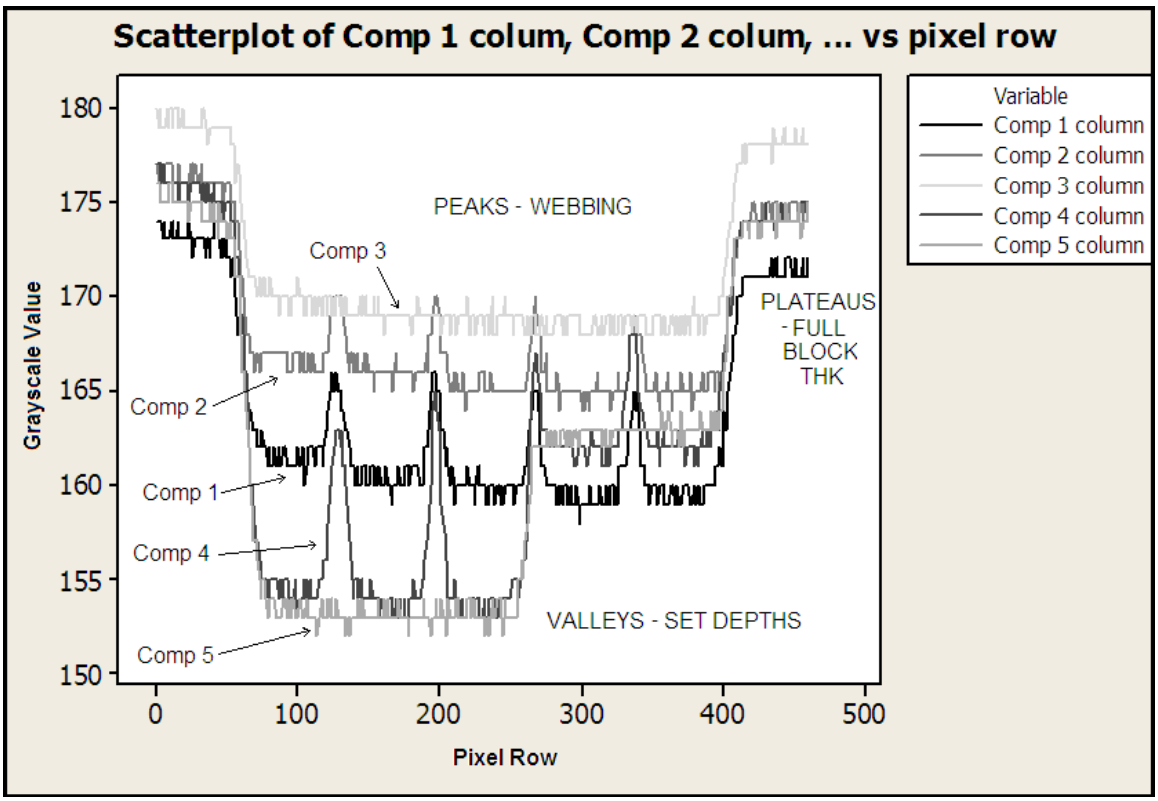

Figure 4.6: Scatterplot of central columns of pixels from all 5 compensators

4.4 Descriptive Statistics

The statistical tests, referring to the paired t-tests and ANOVA summaries listed in *Appendices D and E*, proved that the results from the testing sequence are not statistically the same. However, there are observed similarities that may be seen in *Appendix F*. The scatter plot in *Figure 4.6* shows a visual of the un-adjusted, or un-normalized, data for all five compensators. The y-axis in the scatter plot was the grayscale value derived from the .tif image pixels. The scatter plot may be used to compare the dose-distributions of the five compensators.

The scatter plot, as shown in *Figure 4.6*, indicated that the compensators have many descriptive and observed similarities. The plateaus shown in the scatter plot indicated the intensity fluctuation from compensator to compensator. The specimens were physically identical in the locations depicted by the plateaus if the plateaus were dosimetrically aligned. If the difference between the dose-compensation value of water and acrylic were considered in the creation of the specimens, the valleys of the scatter plot would be aligned dosimetrically (refer to *Figure 4.6*).

The scatter plot can be used to visually compare the effect of the webbing found on compensators 1 (fluid design, fluid adjusted to one level), 2 (solid design, webbing present for testing), and 4 (fluid design, fluid adjusted to three levels to be compared to compensator 5). The peaks found on the scatter plot, shown in *Figure 4.6*, may be the product of the photon radiation passing through the webbing structures on the respective compensators. If a webbing structure can be tolerated in a given treatment plan, the webbing for fluid is the same as the webbing for a solid design as indicated in the scatter

plot. The beam intensity would cause the overall compensator distributions to be slightly offset from each other.

The most important part of the current thesis study was based upon the effectiveness of the ability to control the dosimetric effect that a fluid has on radiation. The scatter plot in *Figure 4.6* indicates the fluid-based compensator can be used to adjust the compensation level of a photon radiation beam. A key point considered while comparing the data was that water and acrylic do not have the same dosimetric value. While conversing with Dr. Chihray Liu, the chief of physics at Shands Cancer Center, Dr. Liu explained that the use of water and acrylic, in equal physical proportions, would not produce the exact same dosimetric value (Dr. C. Liu, personal communication, March, 2010). In other words, the fluid-based compensators and the solid compensators used in the current study were geometrically the same, but have two different dosimetric values. Dr. Liu continued by noting that the column of acrylic has a greater compensation value than water; which means that more water is required to equal the dosimetric value of the acrylic material. Dr. Liu noted that using the same geometric proportions for the current test would yield different results; but, would show a good representation of the similar features of the two designs (fluid design versus solid design).

CHAPTER 5: DISCUSSION

5.1 Restatement of Problem

The purpose of the current research was to conduct a feasibility study exploring an alternate method for creating a proton compensator that implements the use of fluid. Currently, proton compensators are made of solid materials, but an interest in creating a proton compensator using fluid arose to address a need for cost and time efficiency. An increase in demand for proton radiation therapy has resulted in a drive for new technologies that allow for more patients to be treated; and at a more economical price. While collaborating with the University of Florida, and Shand's Cancer Center, a team of Western Carolina University's (WCU) engineering personnel discussed an interest in designing a proton compensator that can be quickly adjusted to meet the needs of various patients' prescribed radiation treatments. While visiting the proton facilities in Jacksonville, Florida, WCU's engineers noted the current method for creating proton compensators consisted of machining blocks of Lucite® to meet pre-determined geometry specified by a radiation physicist. The current method for creating proton compensators takes a minimum of 35-75 minutes for smaller compensators. Larger compensators sometimes take up to several hours to fabricate. Richard Helmig, a reputed medical tooling designer and fabricator working in conjunction with the University of Florida, explained that proton radiation experts agree that a more timely method for creating proton compensators would be highly valued in the field (R. Helmig, personal communication, April, 2009). Larger compensators sometimes take up to several hours to fabricate. In respect to the need for a more cost and time-effective compensator,

speculation of using a fluid-based compensator to replace the conventional proton compensator has developed.

In situations where a tumor is extremely progressive, a doctor may have problems with the time necessary for a compensator to be fabricated. Some proton therapy facilities have the capability to make a portion of their prescribed compensators in-house, but a large percentage of compensators are outsourced. In some cases, a patient may undergo a 3D scan in preparation for radiotherapy only to be disappointed to learn the tumor has progressed into a different shape before the compensator could be fabricated for treatment. A fluid-based design is expected to allow doctors to quickly "dial up" a dose within a matter of minutes. Though the fluid-based design concept seems feasible, no physical groundwork has previously been documented that indicates a fluid-based proton compensator is feasible. The fluid based concept needed to be proved effective in real-world tests to validate theoretical speculation.

5.2 Analysis of Statistical and Descriptive Results

The statistical results of the current study indicated that the fluid-based compensators, in the current dosimetric configuration, are statistically different than the conventional compensators. The descriptive comparisons, such as those shown in *Appendix F*, portray qualities associated with the ability to adjust the compensation level with the fluid-based design. As discussed in *Chapter 4*, there are details that distort the clarity of the statistical results. With such low p-values for the statistical tests, and apparent similarities within the descriptive results, an un-accounted variable may be having an effect on the current data. As previously discussed in *Chapter 4*, radiation fluctuation from the source, and the lack of a consistent orientation during the irradiation

of the specimens were likely the most influential source of variation in the data resulting in p-values of 0.000 at a 95% confidence interval. The inconsistency in the exact repeated orientation of the specimens could have jeopardized the accuracy of the statistical tests (Attix, 2004). The p-values would probably been higher if the part orientations were consistent. If the specimens had been aligned in a consistent fashion, the results may have shown more similarities as shown in the descriptive results. The impact of scattering photons could be an influencing factor if present in the current test, but the current test does not account for the influence of scattering (Greening, 1985). Photon radiation could likely be scattering when encountering the compensators due to natural dosimetric effects (Attix, 2004). The presence of the o-rings on the plugs may have caused additional scatter, which may account for a portion of the grayscale pixel values that fall between the dosimetric response caused by the plugs (denoted as "valleys" on the scatter plot in *Figure 4.6*) and the dosimetric response caused by the full-body thickness of the compensators (denoted as "plateaus" on the scatter plot in *Figure 4.6*). The amount of radiation that scatters was based on multiple factors including the amount of photon energy emitted and the angle in which the interaction occurred (Greening, 1985).

5.3 Conclusive Discussion of Thesis Statement

The objective of the current research effort was to determine the feasibility of creating an experimental proton radiation compensator design, which implements the use of fluid, in place of conventional designs that are currently implemented in the field of proton radiation therapy. The results of the current study suggested that the fluid-based compensator design may be used to control the fluid levels (refer to *Figure 4.6*). As a

result, the dosimetric levels can be adjusted to meet a prescribed compensation value; however, there are currently multiple sources of variance in design (which may be due to the design and/or the testing design). The statistical results of the current study reflect that there is a statistical difference in the dosimetric values of acrylic and water mediums (refer to *Appendices D and E*). From a treatment perspective, improvements concerning the percentage of uncontrollable area could be reduced. The current adjustable areas are circular in shape; and the use of a hexagonal chamber would allow the cross sectional area to be reduced. The benefit of a fluid-based design, in terms of speed, could possibly out-weigh the drawbacks of the design (R. Helmig, personal communication, July, 2009). More tests should be conducted, and the design refined, prior to using the current technology in the field of radiation therapy. Bo Lu, M.S., instructor in radiation oncology at Shands, explained how the initial results of the testing sequence seemed to be effectively controlling the dosimetric value of the particle radiation. Mr. Lu commented that the next evolution in design that he would like to see is to minimize the size of the webbing structure that separates the columns of fluid in order to minimize the uncontrollable area during a treatment (B. Lu, M.S., personal communication, April, 2010).

5.4 Future Testing Scope

The optimization of the testing method used in the current study has room for improvement. For future work, the specimens need to be registered to a precise location on the radiation equipment. The precise mounting would allow for an effective blocking approach for the statistical analysis used in the current study. The "hot spots," as discussed in section 4.3, could be accounted for by blocking if the locations of the spots

do not migrate. To determine the location, and repeatability characteristics of the spots, a pilot test test sequence should be conducted to determine the variance of the machine. One possible way to analyze the fluctuation is to use sheets of precision-cut acrylic as specimens. The specimens would be large enough to cover the entire field of radiation exposure. Operators could irradiate the specimens repeatedly and check for hot spots within the field; and the repeatable nature of the spots. If a baseline could be established, a proper blocking diagram may prove more effective in a statistical test (Box, 2005).

The current study used a sampling method in an effort to normalize the data by the values of an individual hole. The sample area used was square-shaped. In order to achieve a better representation of the sampling area, a circular area should be used to achieve a better representation of the value of a circular feature.

Afterthoughts of the image-processing portion of the current research suggested that the use of the tag image file format (.tif) to save the results, prior to converting the images to a grayscale value, was not the best option. Future experiments should make use of a RAW image file format when saving the results from the initial irradiation test. A RAW image format saves data from an optical sensor with minimal processing of the actual data available. Dr. Peter Tay, an image processing expert at Western Carolina University, explained that file formats, such as .tif, takes the initial sensor data and averages the data values; where a .raw file maintains the data in more detail (Dr. P. Tay, personal communication, April, 2010). For example, a .raw image might save a pixel value to a value of 154.2879; where a .tif image might save the same value as 154. The use of .raw files in future experiments could allow a better analysis of the specimens.

5.5 Future Design Scope

Through the duration of the current study, multiple ideas have been generated that could be implemented into a future design for a fluid-based proton range compensator. The first design change to consider, especially from a dosimetric stand point, would be to change the shape of the fluid chambers. The current design consists of round holes in which a round plug is used to adjust the fluid level. The use of round holes creates an "un-adjustable" area that is undesirable, but not necessarily unacceptable, from a treatment stand point (R. Helmig, personal communication, July, 2009). A hexagonal hole shape is recommended for future chamber designs to decrease the amount of un-controllable space. As shown in *Figure 5.1*, the use of hexagonal holes would increase the usable treatment area, but would likely be more difficult to manufacture.

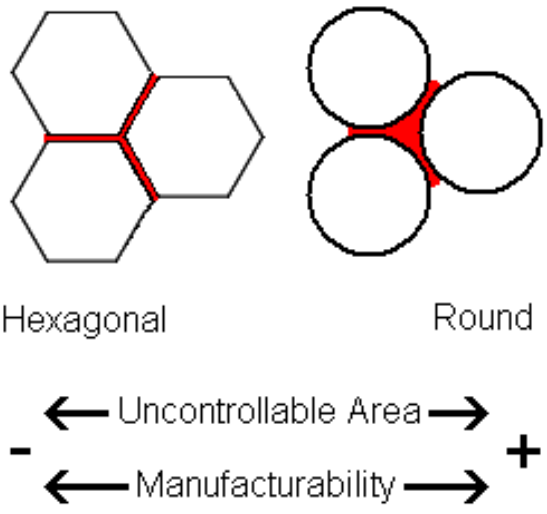

Figure 5.1: Hexagonal holes compared to round holes

The weep hole used in the current fluid compensator design could also be improved. The weep-hole proved to be effective in allowing water to pass through when intended, and not pass through when unwanted. The weep hole design could be avoided if the bottom of all of the fluid chambers coincided into one fluid chamber, with no weep holes. Instead of "weeping" out of the compensator, the fluid could exit the compensator by flowing into a bladder. Ideally, the bladder could have pressure applied to push a previously-set series of plugs back up to a default position. The illumination of the weep-hole design could allow faster, and more robust, fluid level adjustments. Also, the elimination of the weep hole allows less machining time to be spent drilling the intricate holes.

Inserting the plugs into the main compensator housing proved difficult. A slight chamfer was applied to the top of the compensator to aid in the insertion of the plugs. The plug design was primarily based off of the manufacturing capability of the current study as explained in *Chapter 4*. The o-rings may have caused scatter during photon irradiation, but would be less likely to have as much scatter if introduced to proton radiation (Dr. P. Sanger, personal communication, April, 2010). Future designers should attempt to avoid the use of o-rings if possible.

APPENDICES

APPENDIX A: PROTOTYPE DESIGN

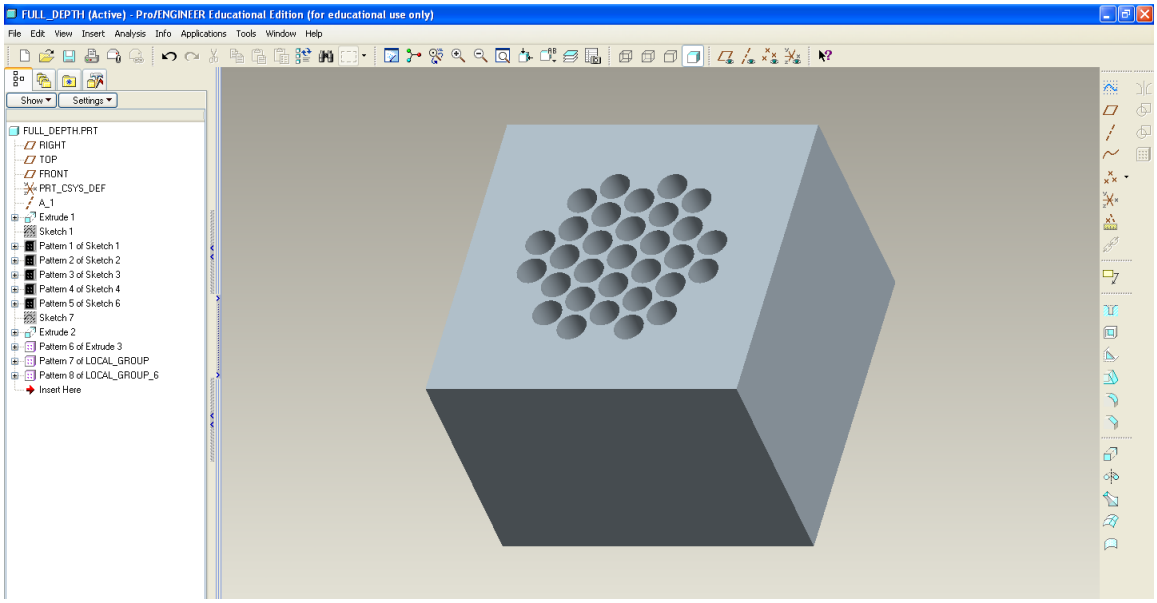

3D constraint-based solid model of compensator

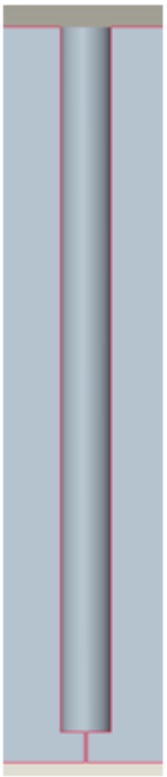

Cross-section view of fluid chamber with weep hole

Acrylic plug with o-rings

APPENDIX B: FABRICATION OF PROTOTYPES

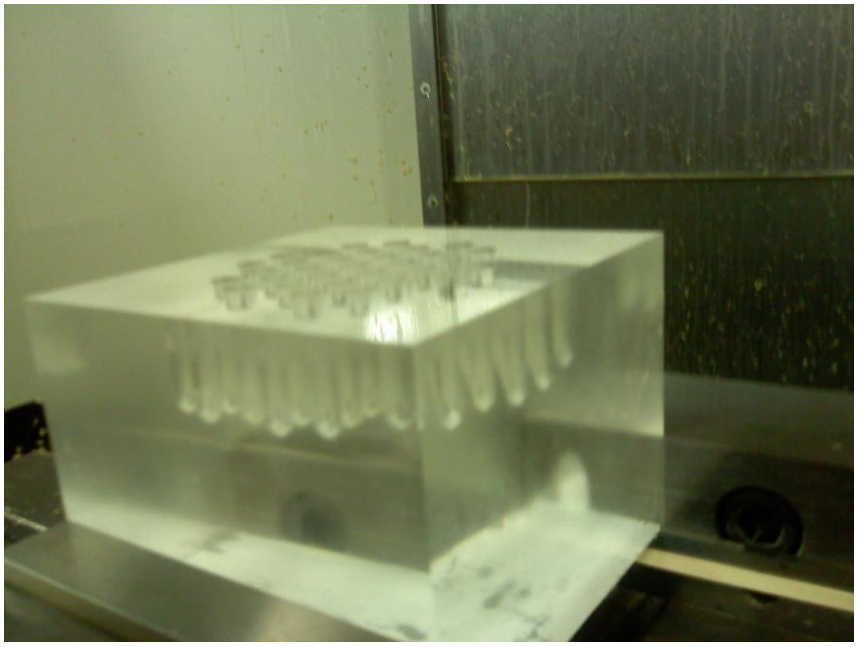

Compensator mounted in CNC machine vice

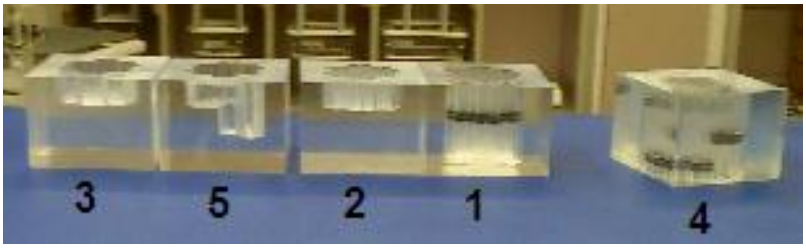

Compensators completed

CNC Mill

CNC Lathe

APPENDIX C: RADIATION TESTING

Compensator testing setup

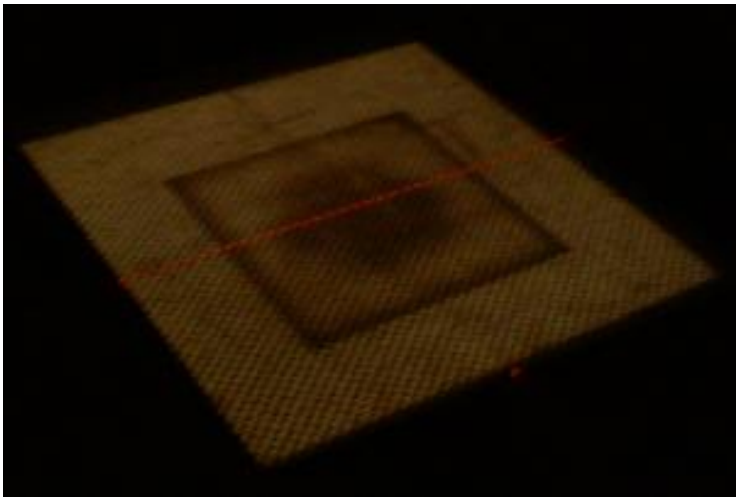

Compensator alignment for testing

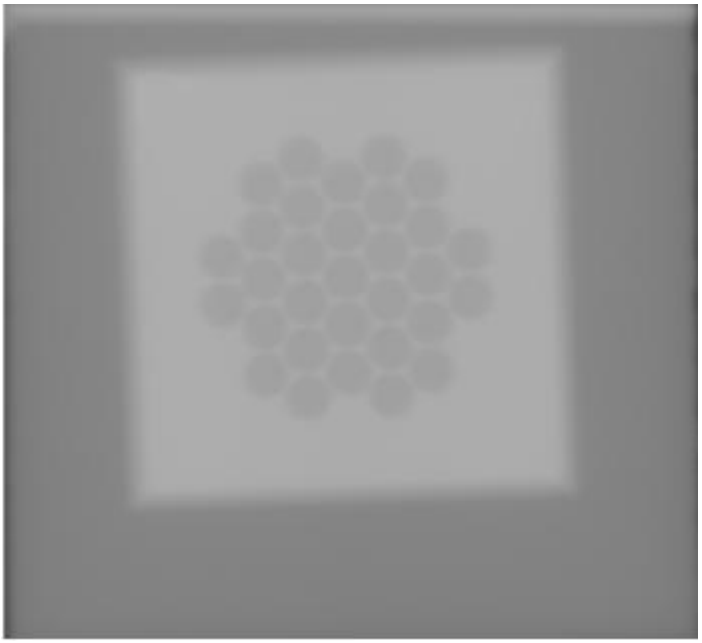

Compensator 1 – original .tif image

Compensator 2 – original .tif image

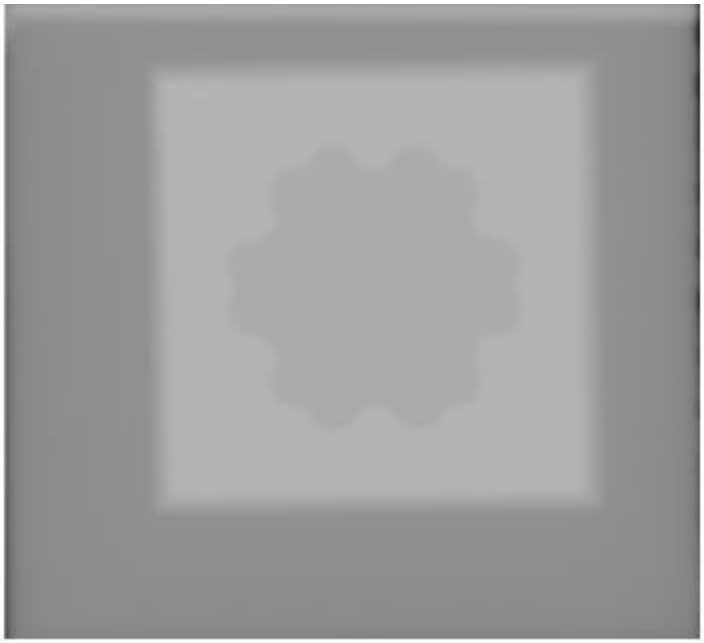

Compensator 3 – original .tif image

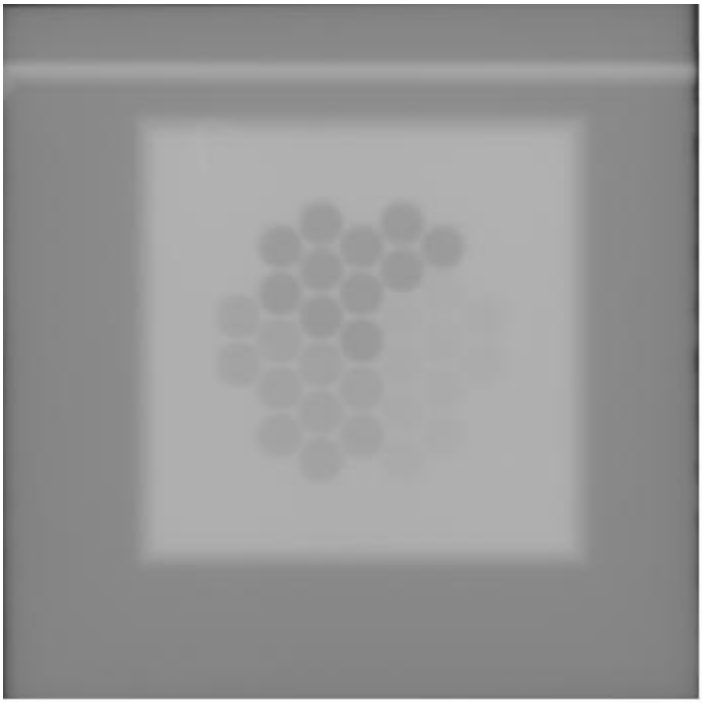

Compensator 4 – original .tif image

Compensator 5 – original .tif image

Compensator 1 – aligned .tif image

Compensator 2 – aligned .tif image

Compensator 3 – aligned .tif image

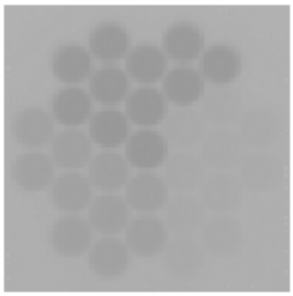

Compensator 4 – aligned .tif image

Compensator 5 – aligned .tif image

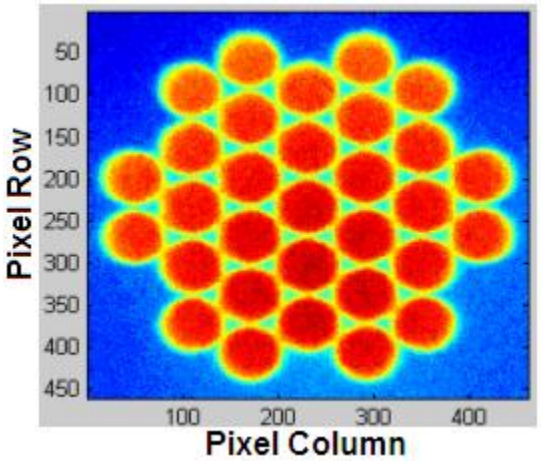

Compensator 1 – aligned and enhanced .tif image

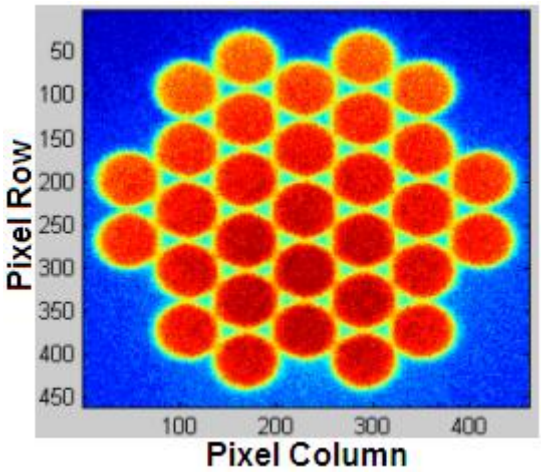

Compensator 2 – aligned and enhanced .tif image

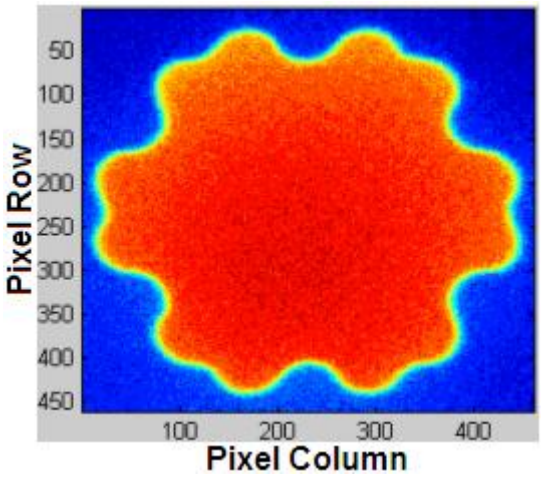

Compensator 3 – aligned and enhanced .tif image

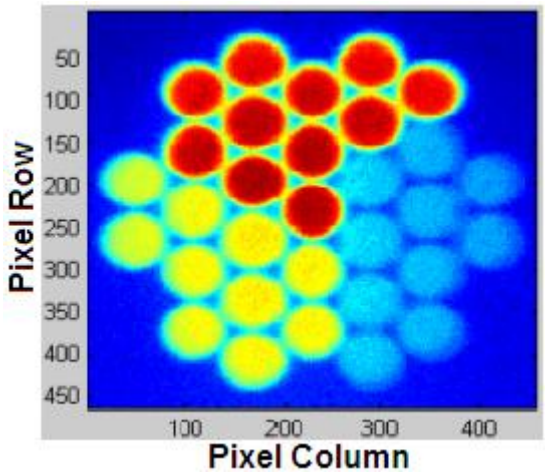

Compensator 4 – aligned and enhanced .tif image

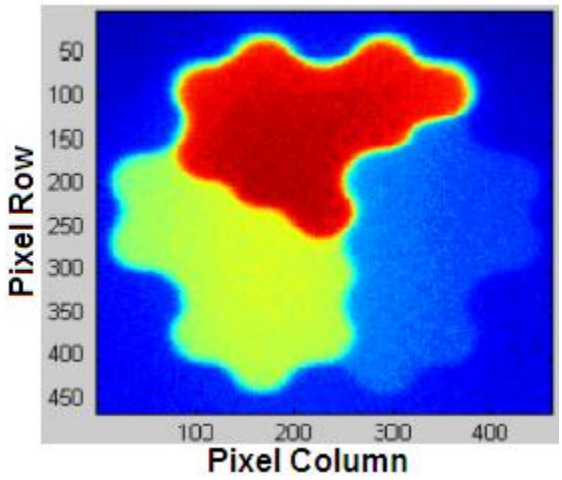

Compensator 5 – aligned and enhanced .tif image

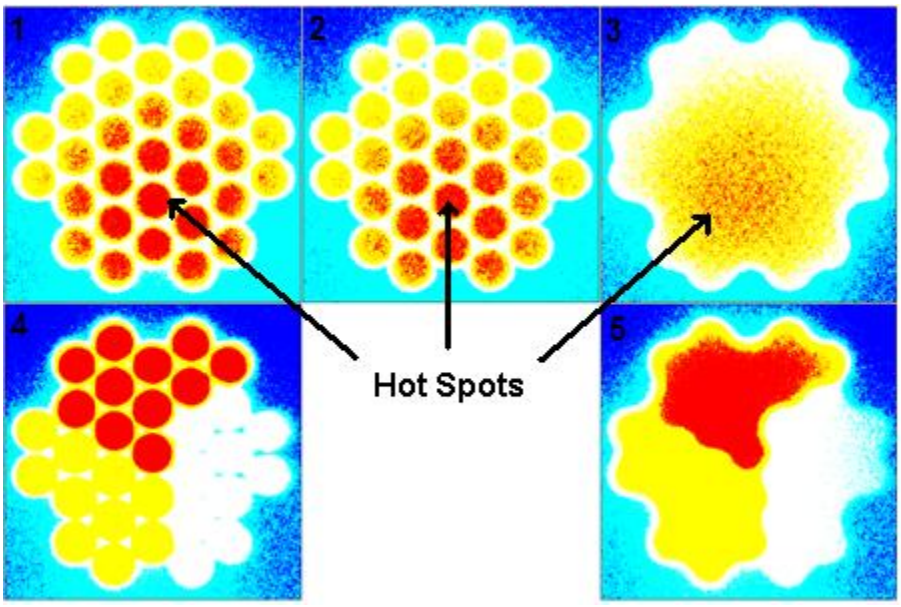

Aligned and enhanced .tif images to illustrate suspected radiation inconsistency

APPENDIX D: STATITISTICAL RESULTS BEFORE NORMALIZATION

Paired T for Specimen1 - Specimen2

	N	Mean	StDev	SE Mean
Specimen1	211600	166.670	5.244	0.011
Specimen2	211600	170.663	4.373	0.010
Difference	211600	-3.99233	1.18939	0.00259

95% CI for mean difference: (-3.99740, -3.98726)
T-Test of mean difference = 0 (vs not = 0):
T-Value = -1544.04 P-Value = 0.000

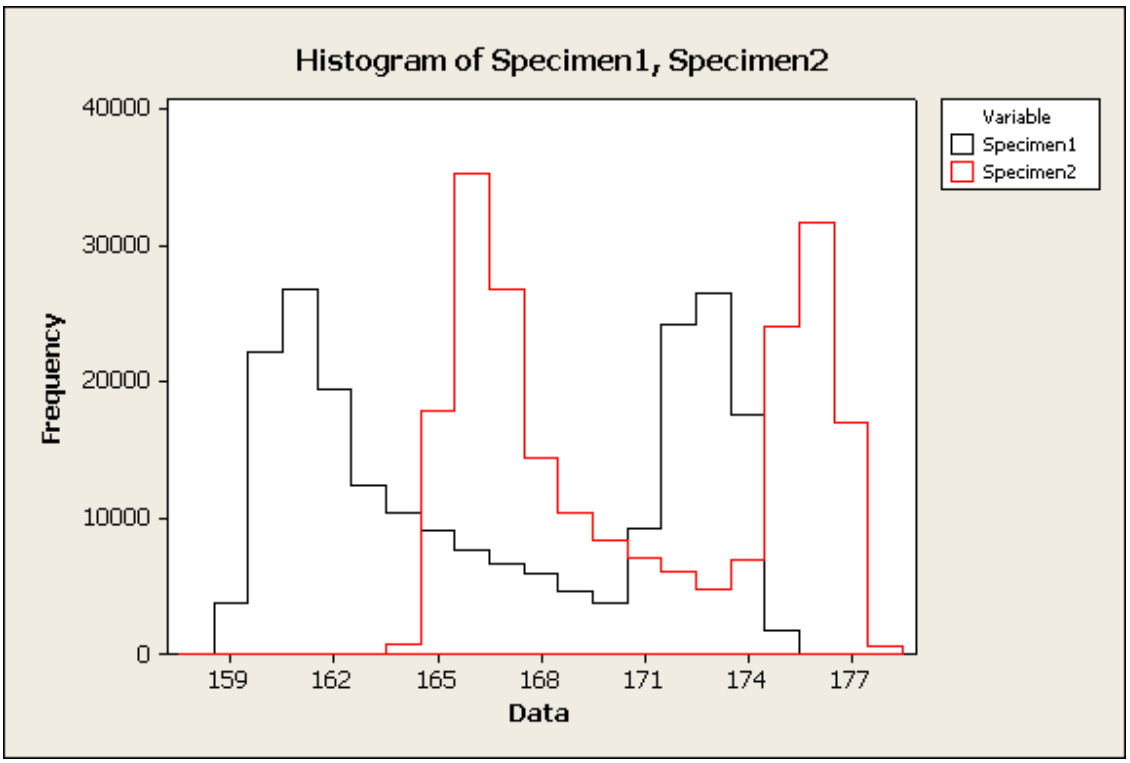

Paired T for Specimen2 - Specimen3

	N	Mean	StDev	SE Mean
Specimen2	211600	170.663	4.373	0.010
Specimen3	211600	173.312	4.667	0.010
Difference	211600	-2.64913	1.74027	0.00378

95% CI for mean difference: (-2.65654, -2.64171)
T-Test of mean difference = 0 (vs not = 0):
T-Value = -700.23 P-Value = 0.000

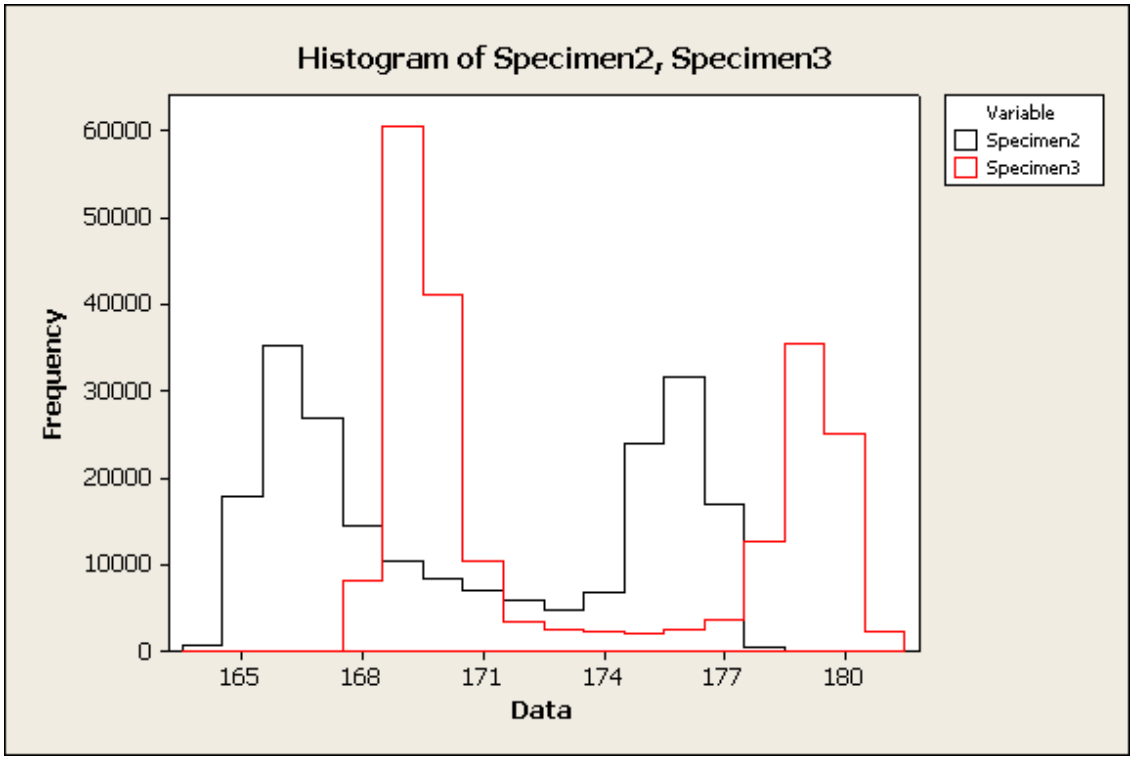

Paired T for Specimen4 - Specimen5

	N	Mean	StDev	SE Mean
Specimen4	211600	168.867	7.083	0.015
Specimen5	211600	168.055	8.069	0.018
Difference	211600	0.81193	2.84606	0.00619

95% CI for mean difference: (0.79981, 0.82406)
T-Test of mean difference = 0 (vs not = 0):
T-Value = 131.23 P-Value = 0.000

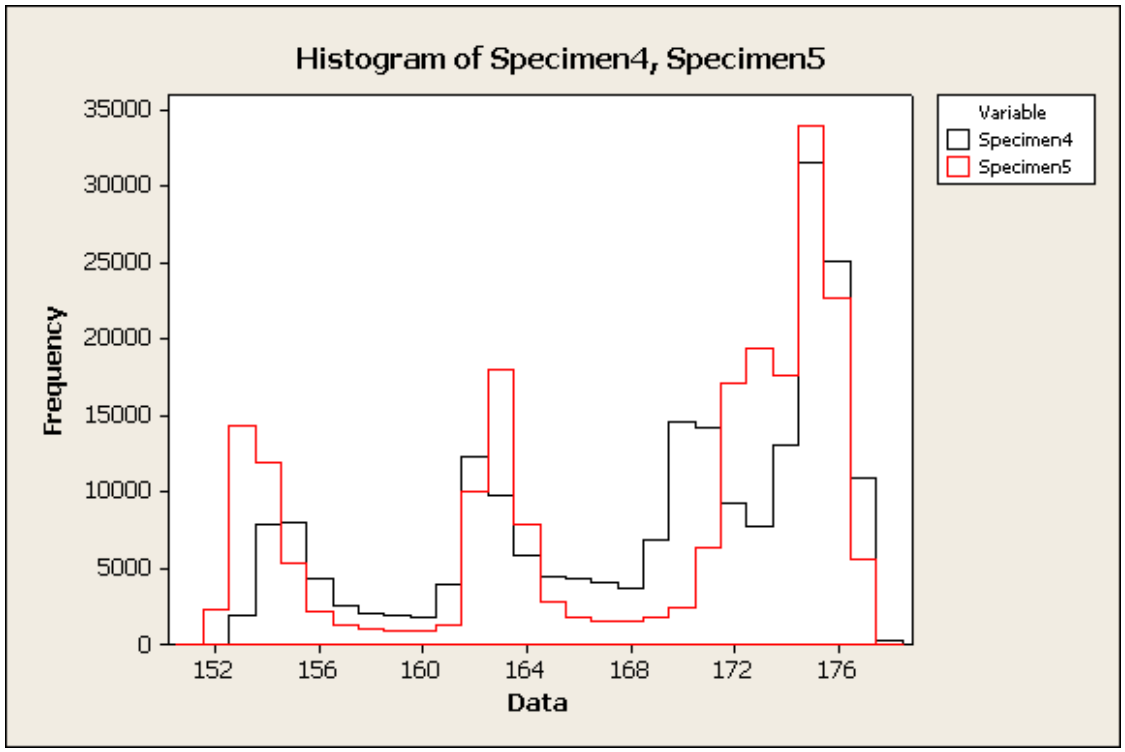

APPENDIX E: NORMALIZED DATA ANALYSIS

One-way ANOVA: adj for full depth versus Compensator

```
Source         DF        SS        MS        F      P
Compensator     2  5123.101  2561.550  3205.59  0.000
Error        4647  3713.361     0.799
Total        4649  8836.461
S = 0.8939   R-Sq = 57.98%   R-Sq(adj) = 57.96%
                             Individual 95% CIs For Mean Based on
Pooled StDev
Level     N     Mean  StDev    --+---------+---------+---------+-------
1      1550  163.733  1.097    (*)
2      1550  165.956  0.814                                        (*)
3      1550  165.963  0.729                                        (*)
                               --+---------+---------+---------+-------
                             163.80    164.40    165.00    165.60
Pooled StDev = 0.894
Tukey 95% Simultaneous Confidence Intervals
All Pairwise Comparisons among Levels of Compensator
Individual confidence level = 98.07%
```

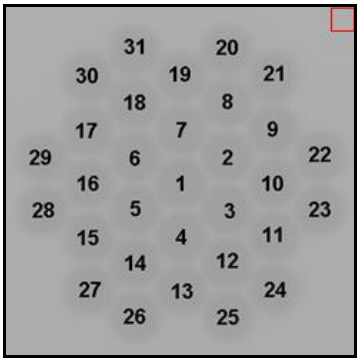

The data was normalized by adjusting the mean values by the difference in the grayscale values at the location shown above

One-way ANOVA: Adj Grayscale for Material Diff versus Compensator

```
Source         DF        SS       MS       F      P
Compensator     2   279.291  139.645  174.76  0.000
Error        4647  3713.361    0.799
Total        4649  3992.651
S = 0.8939   R-Sq = 7.00%   R-Sq(adj) = 6.96%
                             Individual 95% CIs For Mean Based on
                             Pooled StDev
Level     N     Mean  StDev  ---------+---------+---------+---------+
1      1550  165.673  1.097  (--*-)
2      1550  165.956  0.814                (-*-)
3      1550  166.273  0.729                              (--*-)
                             ---------+---------+---------+---------+
                                  165.80    166.00    166.20    166.40
Pooled StDev = 0.894
```

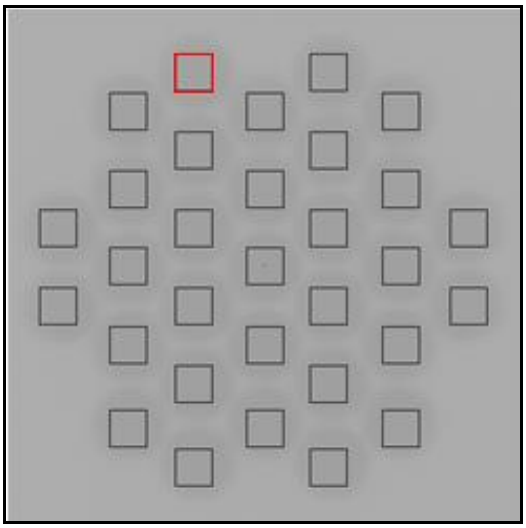

The data was normalized by adjusting the mean values by the difference in the grayscale values at the location shown above.

The following data lists the outcome of a blocked ANOVA to check for variance from hole to hole:

Analysis of Variance for Adj Grayscale for Material Diff, using Adjusted SS for Tests

Source	DF	Seq SS	Adj SS	Adj MS	F	P
Compensator	2	279.29	279.29	139.65	236.80	0.000
Hole	1	973.50	973.50	973.50	1650.76	0.000
Error	4646	2739.86	2739.86	0.59		
Total	4649	3992.65				

S = 0.767936 R-Sq = 31.38% R-Sq(adj) = 31.33%

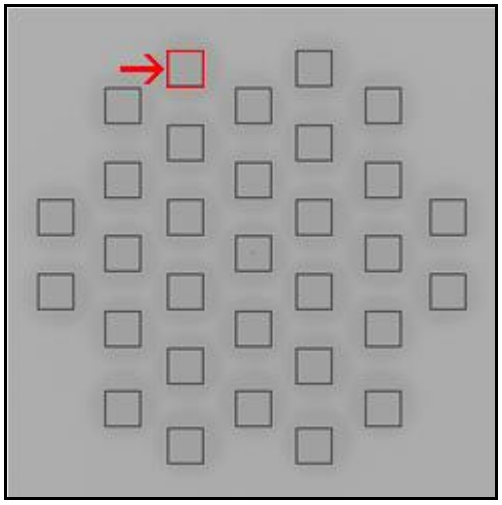

The data was normalized by adjusting the mean values by the difference in the grayscale values at the location shown above

APPENDIX F: DESCRIPTIVE RESULTS

The following section lists a two-sample t-test that compares the pixel values indicated in the image below for compensators 1 and 2. The intent was to avoid the impact of the webbing:

Two-sample T for comp 1 adj to 2 vs comp 2_1

	N	Mean	StDev	SE Mean
comp 1 adj to 2	175	165.314	0.934	0.071
comp 2_1	175	165.606	0.809	0.061

Difference = mu (comp 1 adj to 2) - mu (comp 2_1)
Estimate for difference: -0.2914
95% CI for difference: (-0.4751, -0.1078)
T-Test of difference = 0 (vs not =):
T-Value = -3.12 P-Value = 0.002 DF = 348
Both use Pooled StDev = 0.8735

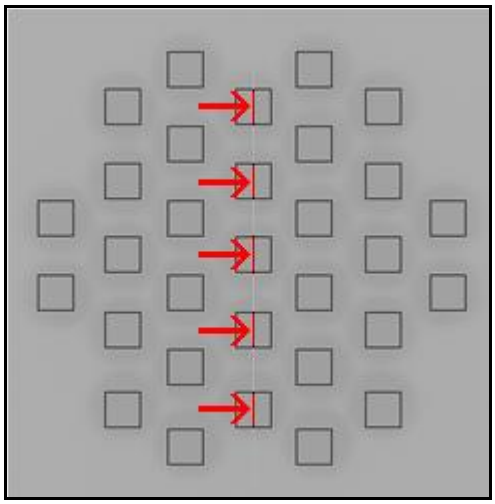

The data for the two-sample t-test above was normalized using the full compensator thickness. The data points included in the analysis included the center column of grayscale values indicated above.

The following image depicts the head-to-head comparison of all of the five compensators. The data is pulled from the pixels associated with the column of pixels indicated in the picture at the bottom of the page:

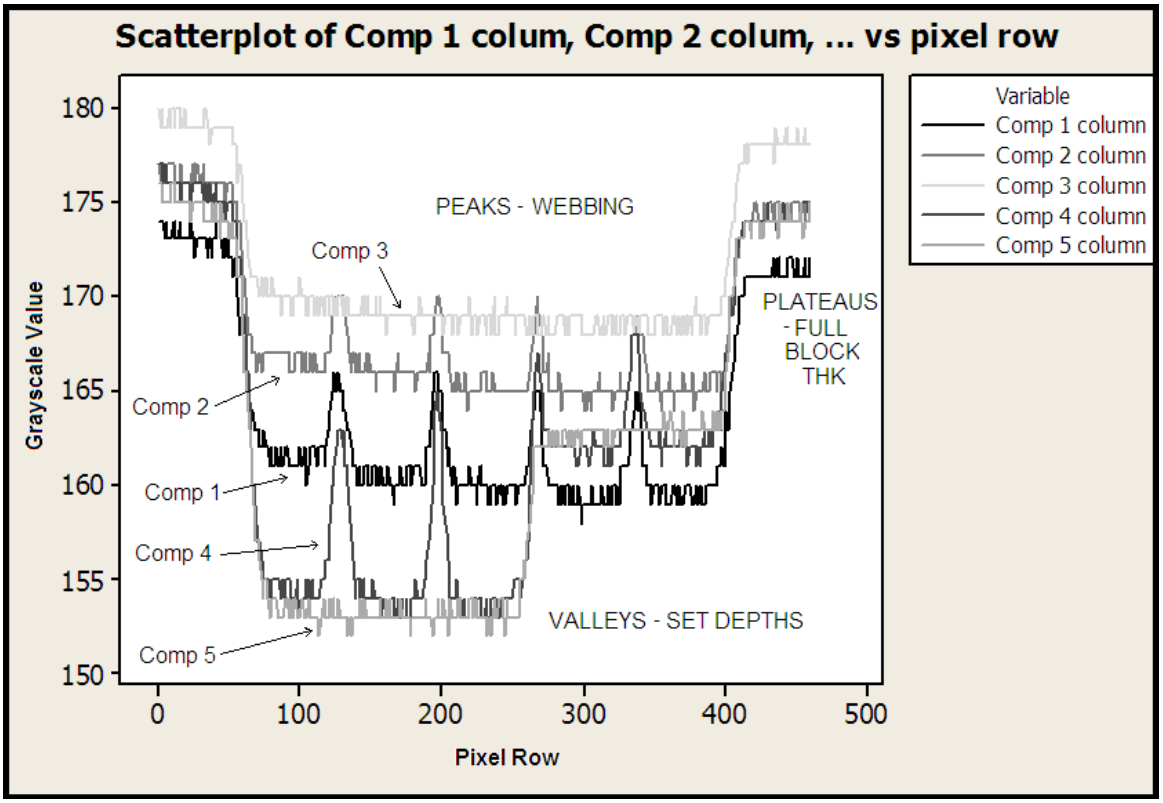

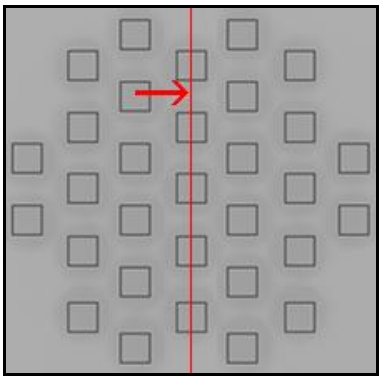

The data illustrated in the scatter plot above consists of the data points indicated in the center column of grayscale values denoted by the line.

APPENDIX G: FUTURE DESIGN SCOPE

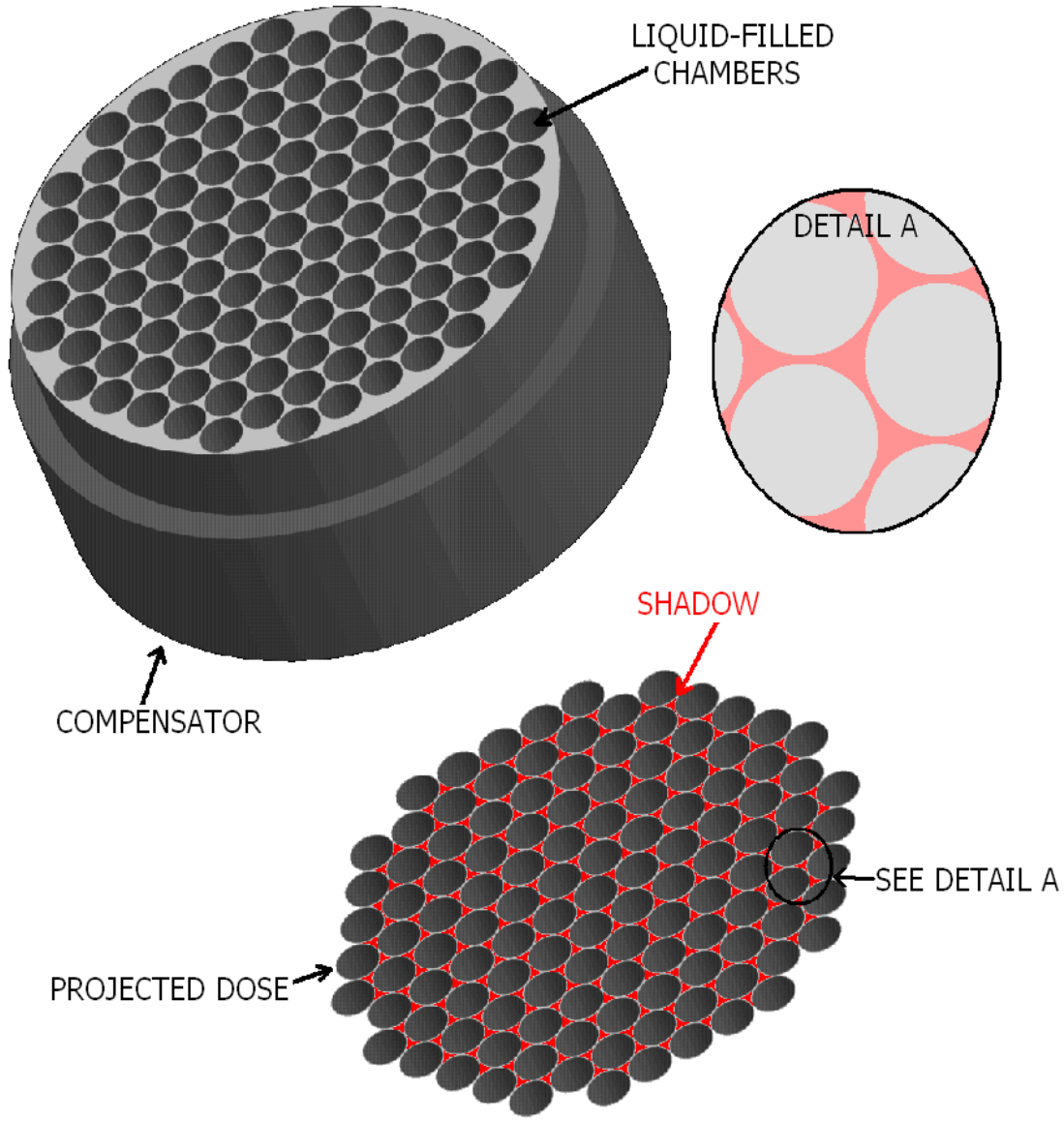

Uncontrolled shadow area due to webbing

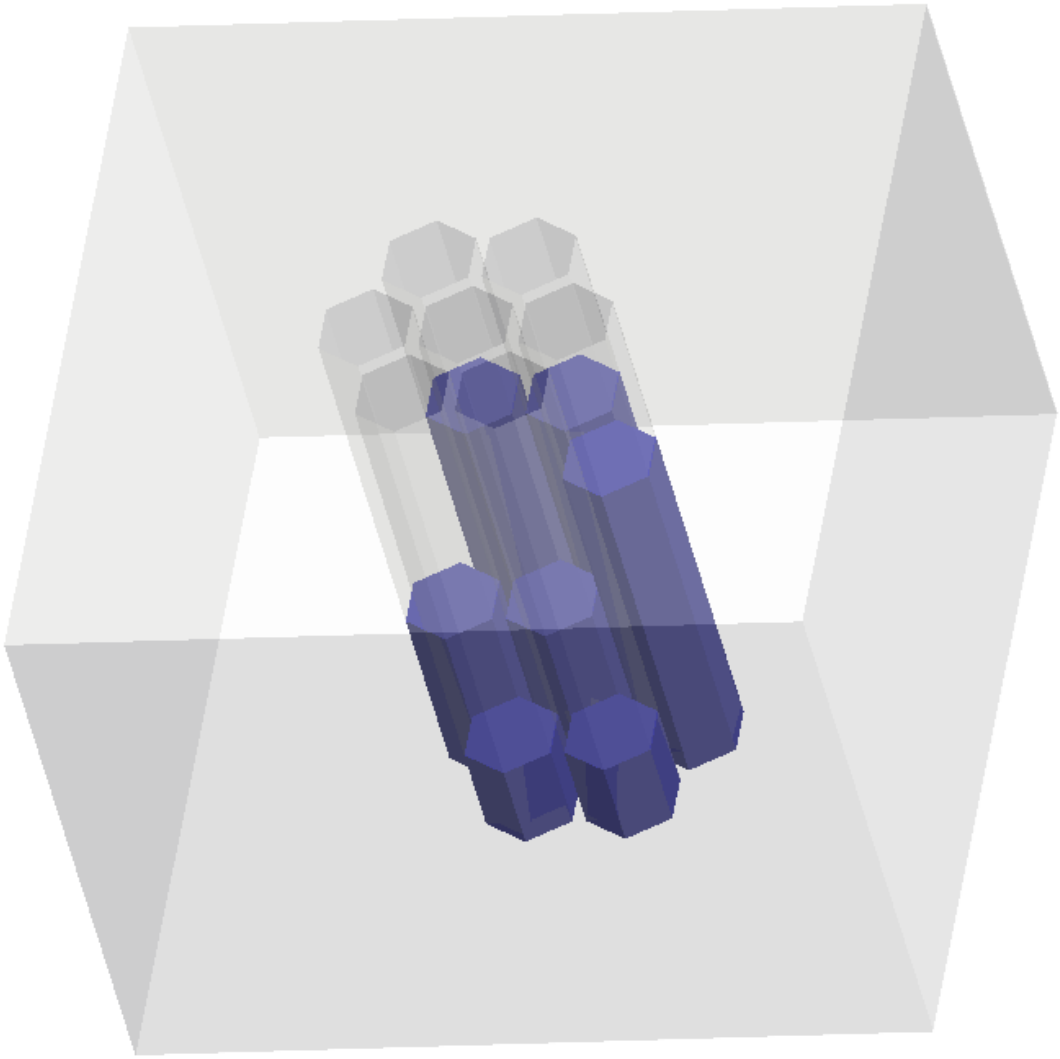

Conceptual view of hexagonal fluid chambers

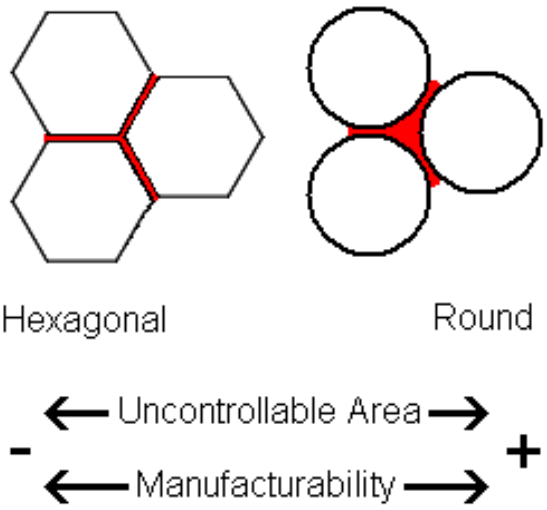

Hexagonal holes compared to round holes

REFERENCES

Advanced Cancer Therapy Foundation (2006). *Science*. Retrieved October 20, 2009, from http://www.advanced-cancer-therapy.org/science_radio.html

Altman, A. J. (Ed). (2004). *Supportive care of children with cancer: Current therapy guidelines from the children's oncology group*. London, England: The Johns Hopkins University Press.

Attix, Frank H., (2004). *Introduction to radiological physics and radiation dosimetry*. Weinheim, Germany: Wiley-VCH Verlag GmbH & Co.

Bates, C. (2006, August 17). The Beam team [Electronic version]. *American Machinist*, Retrieved from: http://www.americanmachinist.com/304/Issue/Article/False/24813/

Box, G. E. P., & Hunter, J. S., & Hunter, W. G. (2005). *Statistics for experimenters: Design, innovation, and discovery*. Hoboken, New Jersey: John Wiley & Sons.

Chui, G. (2008, December 8). The Power of proton therapy [Electronic version]. *Symmetry*, 5, 6.

Cukier, D, and Gengerelli, F., and Makari-Judson, G., and McCullough, V. E. (2004). Coping with chemotherapy and radiation. New York, New York: McGraw-Hill

Freeman, T. (2007, May 8). *Proton therapy up close*. Retrieved November 3, 2009, from http://medicalphysicsweb.org/cws/article/research/29912

Goitein, M., & Jermann, M. (2003). The relative costs of proton and x-ray radiation therapy. *Clinical Oncology (Royal College of Radiologists (Great Britain))*, 15(1), 37-50.

Greening, J. R., (1985). *Fundamentals of radiation dosimetry*. Bristol, England: Adam Hilger Ltd.

International Atomic Energy Agency (2000). *Absorbed dose determination in external beam radiotherapy* (Technical Reports Series No. 398). Vienna, Austria: International Atomic Energy Agency.

Jäkel, O. (2009). Medical physics aspects of particle therapy. *Radiation Protection Dosimetry*, 137(2), 156-166.

Kooy, H. M, & DeLaney, T. F. (Eds.). (2007). *Proton and charged particle radiotherapy* (p. 84). Philadelphia: Lippincott Williams & Wilkins.

Loma Linda University, Medical Center. (2008, October 7). *Proton therapy may significantly reduce risk of developing secondary cancers*. Retrieved October 15, 2009, from the James M. Slater Proton Treatment and Research Center Web site: http://www.protons.com/cancer-resources/news/2008/10/07/proton-therapy-significantly-reduces-risk-of-developing-secondary-cancers.html

Massachusetts General Hospital Cancer Center. (2005). *Northeast Proton Therapy Center* [Electronic Brochure]. Bussière, MR: Author.

Massachusetts General Hospital Cancer Center, Department of Radiation Oncology, Harvard Medical School. (2005). *Principles of proton therapy [Electronic Brochure]*. Bussière, Marc R.: Author.

Mozumder, A. (1999). *Fundamentals of Radiation Chemistry*. San Diego, California: Academic Press.

U.S. National Institutes of Health. (2004, August). *Radiation therapy for cancer: Questions and answers*. Retrieved March 10, 2010, from National Cancer

Institute Web site: http://www.cancer.gov/cancertopics/factsheet/Therapy/radiation

Novikov-Borodin, A. V. (2009, December 12). *Advantages of protons for radiotherapy*. Retrieved from: http://www.medphysics.inr.ru/

Schiff, D., & D'Agostino, R. (1996). *Practical Engineering Statistics*. New York, New York: John Wiley & Sons

The National Association for Proton Therapy (2009). *How It Works*. Retrieved October 19, 2009, from http://www.proton-therapy.org/howit.htm

University of Florida, Proton Therapy Institute. (2006). *Targeting Tumors*. Retrieved October 3, 2009, from the University of Florida's Proton Therapy Institute's Office of Research Publications Web site: http://www.floridaproton.org/pdf/ExploreF06_proton.pdf

University of Florida, Proton Therapy Institute. (2009). *The Terms of Cancer Treatment: Common cancer terminology explained*. Retrieved November 3, 2009, from the University of Florida's Proton Therapy Institute's Office of Research Publications Web site: http://www.floridaproton.org/cancer-treatment/terminology.html

University of Florida, Proton Therapy Institute. (2009, July). *How Proton therapy works*. Retrieved September 7, 2009, from the University of Florida's Proton Therapy Institute's Office of Research Publications Web site: http://www.floridaproton.org/pdf/how_it_works_rev_7.09.pdf

University of Tsukuba, Proton Medical Research Center. (2007). *Proton beam radiotherapy*. Retrieved November 3, 2009 from the Proton Medical Research Center Web site: http://www.pmrc.tsukuba.ac.jp/engBeam.html